 doi:10.20944/preprints202104.0577.v1

Article

Climate change projections of dry and wet events in Iberia based on the WASP-Index

Cristina Andrade [1,2]*, Joana Contente [1] and João A. Santos [2]

[1] Instituto Politécnico de Tomar, Natural Hazards Research Center (NHRC.ipt), Quinta do Contador, Estrada da Serra, 2300-313 Tomar, Portugal
[2] Centre for the Research and Technology of Agro-Environmental and Biological Sciences (CITAB), University of Trás-os-Montes e Alto Douro, PO Box 1013, 5001-801 Vila Real, Portugal
* Correspondence: c.andrade@ipt.pt; Tel.: +351 249 328 100

Abstract: The WASP-Index is computed over Iberia for three monthly timescales in 1961–2020, based on an observational gridded precipitation dataset (E-OBS), and in 2021–2070, based on bias-corrected precipitation generated by a six-member climate model ensemble from EURO-CORDEX, under RCP4.5 and RCP8.5. The WASP performance in identifying extremely dry or wet events, reported by the EM-DAT disaster database, is assessed for 1961–2020. An overall good agreement between the WASP spatial patterns and the EM-DAT records is found. The areolar mean values revealed an upward trend in the frequency of occurrence of intermediate-to-severe dry events over Iberia, which will be strengthened in the future, particularly for the 12m-WASP intermediate dry events under RCP8.5. Besides, the number of 3m-WASP intermediate-to-severe wet events is projected to increase, mostly the severest events under RCP4.5, but no evidence was found for an increase in the number of more persistent (12m-WASP) wet events under both RCPs. Despite important spatial heterogeneities, an increase(decrease) of the intensity, duration, and frequency of occurrence of the 12m-WASP intermediate-to-severe dry(wet) events is found under both scenarios, mainly in the southernmost regions of Iberia, thus becoming more exposed to prolonged and severe droughts in the future, corroborating the results from previous studies.

Keywords: WASP-Index; Climate change; Projections; Extreme precipitation; Iberian Peninsula

1. Introduction

It is commonly accepted that climate change has a direct link to the increasing frequency and intensity of extreme events [1]. The projected increases in temperature [2–4] and alterations in the precipitation patterns will be accompanied by more frequent and intense droughts, as well as floods [5]. These extreme events can have a deep impact on the economy [6–8], agriculture [9,10], and the environment [11]. Therefore, a better understanding of their future projections in regions more vulnerable to climatic shifts is of utmost relevance.

Droughts can be defined as a prolonged precipitation absence leading to a deficit in natural water availability [12]. However, four different types of droughts can be defined in an increasing severity grade, namely: meteorological, which is caused by a precipitation deficit with respect to the climatological average of a region; agricultural, which is identified when the soil moisture is scarce to sustain a crop production; hydrological, induced by weak streamflows leading to low water levels in rivers, lakes, and reservoirs; and, lastly, socio-economic, that can be defined as the consequence of the above-mentioned drought types, conducting to a lack of water supply to produce/sustain an economic good/service [13,14]. Floods are one of the most recurrent natural hazards in the world [15] and can be defined, to a certain extent, as the opposite of droughts, hence an excess of precipitation relative to the climatological average in a given region, promoting a rise of water levels in rivers, lakes, and reservoirs. However, the timescales and spatial extent of

 doi:10.20944/preprints202104.0577.v1

droughts and floods are commonly different, being the former more prolonged in time and covering larger areas, while the latter typically develop in much shorter periods and are often constrained to flood-risk areas.

Changes in precipitation patterns have implications on water availability and, consequently, on its management [16]. Shifts in these patterns combined with an increase in drought and flood frequency may thus exacerbate the hydroclimatic risks. These risks can have a wide range of impacts, depending on the region. In particular, the Mediterranean region, which is frequently considered amongst the most exposed to climate change risks [17–22], is therefore highly susceptible. In the Iberian Peninsula (IP), for example, these risks include an increase in the number and extension of wildfires, mostly in the summer, an increase in the intensity and duration of droughts [23,24], as well as an increasing number and intensity of winter storms (Xynthia in 2010; Dirk in 2014; Leslie in 2018; Elsa, Fabien and Gloria in 2020) that promote floods and flash floods [25]. Additionally, the precipitation regimes in Iberia are characterized by strong irregularity and inter-annual variability related to persistent large-scale eddies in the eastern North Atlantic [26,27], associated with jet stream wave-breaking episodes [28,29].

Several climatic indices can be used to assess floods and drought events and, consequently, wet and dry events, namely the Standardized Precipitation Index (SPI), Standardized Precipitation Evapotranspiration Index (SPEI), Standardized Precipitation Temperature Index (SPTI), Rainfall Variability Index (RVI), and Weighted Anomaly of Standardized Precipitation Index (WASP-Index). In this study, wet and dry events will be assessed by using the WASP-Index. This index was first proposed by [30] and is based on the previous formulation presented by [31]. Several studies used this index that proved to be a useful tool to assess dry events. [32] used this index in the IP; [33] for Romania; [34,35] for Sri Lanka; [36] for Pakistan; [37] on a global scale; [38] for the Middle East, and [11] reviewed drought-related catastrophes worldwide. An assessment of the impact of hydroclimatic events on the economic growth in sub-Saharan Africa was made by [6], while [39] analysed the impacts of rainfall shocks in Ethiopia. [7] used this index to make an empirical analysis on the effects of climate hazards on national-level economic growth, while [8] compares European countries with different economic developments. [40] used this index to assess inter-annual precipitation variability and crop yield in Nigeria, while [34] assess drought hazard risk in Sri Lanka throughout the WASP-Index.

This study is an extension of [32] work in which the severity, frequency, and spatial variability of droughts in IP were assessed for three different time scales (3-, 6- and 12-months), using four observational precipitation-gridded data sets. Furthermore, the WASP-Index and SPI were also compared in the preceding study, and it was concluded that both indices are highly correlated for this region. Therefore, the main purpose of the present study is to use only the WASP-Index as an indicator for intermediate-to-severe wet and dry events. As previously, the WASP-Index is computed on three different time scales (hereafter, 3m-WASP, 6m-WASP, and 12m-WASP) from 1961 to 2070. Though the WASP-Index is computed on a monthly timescale, four 30-year climatology's are also analysed: 1961–1990 (baseline climate), 1981–2010 for the recent past period using an observation-based dataset; and projections for the future periods 2021–2050 and 2041–2070, under two Representative Concentration Pathway (RCP) scenarios, RCP4.5 and RCP8.5. Towards this aim, an ensemble of 6-member Regional Climate Models (RCMs) of bias-corrected monthly precipitation data was used to compute the monthly WASP-Index and, hence the respective magnitude (severity), duration, intensity, and probability for the four above-referred 30-year periods. The spatial representation for specific dry and wet events is identified in the EM-DAT database and presented along with projections for the duration, intensity, and probability under RCP4.5 and RCP8.5, and for the four 30-year climatologies.

2. Data and Methodology

2.1-Data and bias correction

Preprints (www.preprints.org) | NOT PEER-REVIEWED | Posted: 21 April 2021 doi:10.20944/preprints202104.0577.v1

Observation-based gridded daily total precipitation (in mm) from E-OBS, v23.0e, was retrieved from the EU-FP6 project UERRA (https://www.ecad.eu/download/ ensembles/ensembles.php), for the period from January 1961 to December 2020, on a 0.1° regular grid [41]. This dataset was subject to a bilinear interpolation on a 0.11° regular grid, thus allowing an overlap period with the simulated data.

Projections for daily total precipitation were taken from the EURO-CORDEX initiative (https://www.euro-cordex.net), which provides regional climate models for Europe at a 12.5 km (EUR-11) resolution, for the periods 1951–2005 (historical) and 2006–2070 (scenarios). The RCMs, along with the respective driving models and contributors, are presented in Table 1. The RCM runs under the RCPs [42,43] were attained from the Coupled Model Intercomparison Project 5 (CMIP5) global climate project [44]. In this study, two RCPs were analysed: RCP4.5, which implies a stabilization without crossing out the pathway to a 4.5 W m^{-2} stabilization after 2100 [45–47], and RCP8.5 that is associated with a rising radiative forcing pathway to 8.5 W m^{-2} in 2100 [48,49].

Table 1. Regional Climate Models (RCMs) and their respective driving models and contributors.

RCM	Driving Model	Contributor
ALADIN53	CNRM-CM5	Météo France, CNRM
HIRHAM5	ICHEC-EC-EARTH	Danish Meteorological Institute, DMI
WRF331F	IPSL-CM5A-MR	Institute Pierre-Simon Laplace, IPSL-INERIS
RACMO22E	ICHEC-EC-EARTH	Royal Netherlands Meteorological Institute, KNMI
REMO2009	MPI-ESM-LR	Max Planck Institute for Meteorology, MPI-CSC
CCLM4-8-17	ICHEC-EC-EARTH	Climate Limited-Area Modelling Community, CLMcom

The bias correction method used in this study was the quantile-quantile method, which assumes that the distribution function of a variable may change in the future, but allows a correction of the whole distribution, with tails included. Details about this methodology are described in [50] and [2].

All subsequent calculations are carried out for the study area, a Euro-Atlantic sector comprising the IP (34.625°N-45.075°N, 15.125°W-4.785°E). It is worth mentioning that all calculations are undertaken for all grid points and will only be clipped for the figures presented herein, thus excluding grid points in the Atlantic Ocean and the Mediterranean Sea (Figure 1). All maps have the GCS ETRS 1989 Geographical Coordinate System.

Preprints (www.preprints.org) | NOT PEER-REVIEWED | Posted: 21 April 2021 doi:10.20944/preprints202104.0577.v1

Figure 1. Iberian Peninsula (IP) study area, with the respective Nomenclature of Territorial Units for Statistics (NUTS) NUTS 2 boundaries.

2.2. WASP-Index calculation

As stated above, the WASP-Index was first proposed by [30], based on the formulation presented by [31]. The WASP-Index is obtained through the following equation:

$$\mathrm{WASP_N} = \frac{\mathrm{SUM_N}}{\sigma_{\mathrm{SUM_N}}} \quad (1),$$

$$\mathrm{SUM_N} = \sum_{i=1}^{N} \left(\frac{P_i - \bar{P}_i}{\sigma_i}\right) \frac{\bar{P}_i}{\bar{P}_A} \quad (2),$$

where P_i is the observed i-th month precipitation attained from daily ensemble-mean precipitation (PR), $\bar{P}_i$ is the precipitation baseline climatology (1961–1990) for the corresponding month/year, σ_i is the standard deviation of monthly precipitation, and $\bar{P}_A$ is the mean annual precipitation. $\mathrm{SUM_N}$ in (2) is obtained considering the preceding N months (time scale of the index). For example, $\mathrm{WASP_{12}}$ is calculated taking into consideration the preceding 11 months of the month that is being calculated. Furthermore, the WASP-Index allows a qualitative classification of dry and wet severity through its values, as described in Table 2.

Table 2. WASP-Index values and their corresponding meaning.

WASP values	Meaning
WASP ≤ -2	Severe dry
-2 < WASP ≤ -1.5	Intermediate dry
-1.5 < WASP ≤ -1	Moderate dry
-1 < WASP < 1	Near normal
1 ≤ WASP < 1.5	Moderate wet
1.5 ≤ WASP < 2	Intermediate wet
WASP ≥ 2	Severe wet

Preprints (www.preprints.org) | NOT PEER-REVIEWED | Posted: 21 April 2021 doi:10.20944/preprints202104.0577.v1

For this study, the WASP-Index was computed for timescales, i.e., 3m-WASP (which has 1318 instants, with the first summing the period from January 1961 to March 1961), 6m-WASP (totalizing 1315 instants, with the first being the sum of the period from January 1961 to June 1961), and 12m-WASP (1309 instants in total, the first encompassing January 1961 to December 1961), for the period between 1961 and 2070. These three indices (3m-WASP, 6m-WASP, and 12m-WASP) were attained from E-OBS (Jan-1961 and Dec-2020) for the past period (1961–2020), and from the bias-corrected ensemble, under RCP4.5 and RCP8.5, from 2021 until 2070. For the past period, the three-time scaled WASP indices were averaged over latitude and longitude to obtain a single time series that will allow the identification of the dry and wet events over the target region.

Furthermore, a comparison between the spatial representation of selected dry and wet events presented in [32], as well as extreme events in the EM-DAT disaster database [25], are presented and discussed in section 3.1.

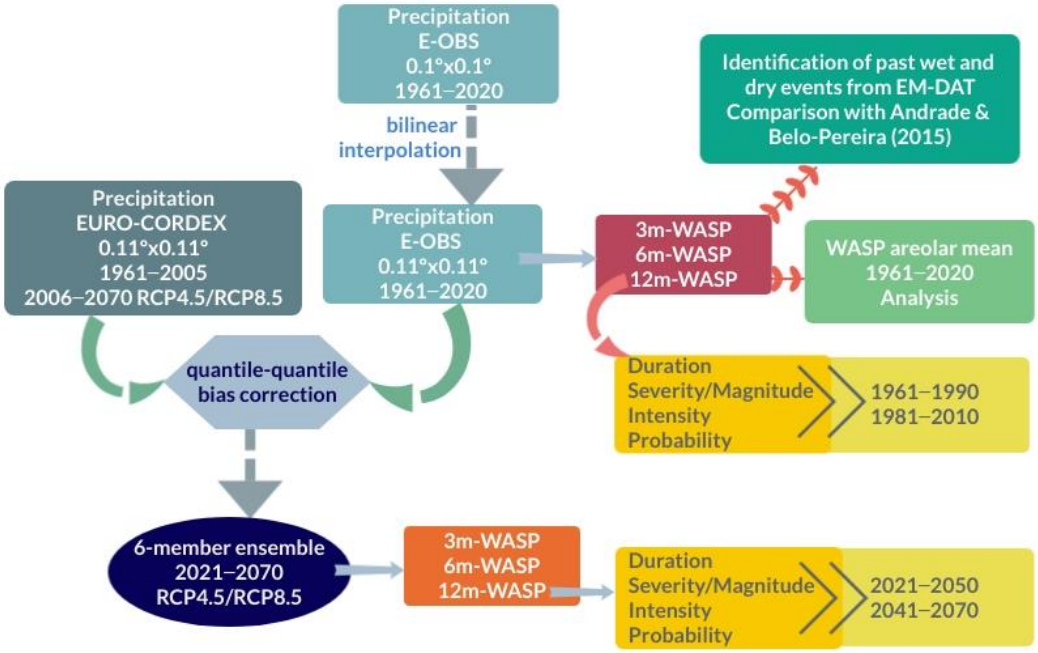

Figure 2. Schematic representation of this study methodology.

2.3. Dry and wet events methodological analysis

The spatial and temporal evolution of wet and dry events is analysed for two mean historical periods, 1961–1990 and 1981–2010 (from the E-OBS dataset), and two future periods, 2021–2050 and 2041–2070 (from the six-member bias-corrected ensemble), under RCP4.5 and RCP8.5, for the 12m-WASP (Figure 2). Towards this goal, the spatial-temporal evolution of duration, intensity, severity, and frequency for these four time periods will be analysed for the IP, as well as for some illustrative main cities.

The duration of an event is determined by the total number of consecutive months for which the index value falls between -2 and -1.5 (1.5 and 2) for intermediate dry (wet), below or equal -2 (above or equal 2) for severe dry (wet) but lasting at least 2 consecutive months to ensure that the extreme event has occurred [51]. In this study, only the results regarding the threshold -1.5 (1.5) for intermediate-to-severe dry (wet) events are presented (≤-1.5 and ≥1.5, respectively).

The severity or magnitude of an event is calculated by:

$$\text{Magnitude} = \sum_{j=1}^{x} 12m - WASP_j \quad (3),$$

Preprints (www.preprints.org) | NOT PEER-REVIEWED | Posted: 21 April 2021 doi:10.20944/preprints202104.0577.v1

where j is the first month in which the 12m-WASP lies below/above a chosen value and x is the month when the 12m-WASP becomes greater/lower than the threshold value [52]. As previously referred, only the results with a threshold smaller or equal to -1.5 (greater or equal to 1.5) for intermediate-to-severe dry (wet) events are analysed.

The intensity is defined as the average index value per month, which is high and has a severe impact when a large magnitude occurs over a short period.

Lastly, the frequency is the probability of occurrence of a dry or wet event (in %), defined by the following equation:

$$\text{Probability } \% = \frac{\text{Total number of dry or wet months}}{\text{Total number of months}} \times 100\% \quad (4).$$

As stated before, only the spatial representations of the results concerning intermediate-to-severe dry (wet) events are presented and discussed (Section 3.2). The overall schematic methodology followed in this study is illustrated in Figure 2.

3. Results & Discussion

3.1. WASP-Index and the EM-DAT disaster database

In this section, several wet and dry events documented by several sources, namely in the EM-DAT disaster database, the European Climate Assessment & Dataset Extreme Events, and [32] will be presented. To facilitate the identification of specific locations displayed in Tables 3 and 4, related figures will have superimposed the NUTS 2 boundaries for Spain (ESP) and Portugal (PRT) previously shown in Figure 1. The events are described in a chronological sequence, for intermediate-to-severe wet (Table 3, Figure 4) and dry (Table 4, Figure 5) events, respectively. In Tables 3 and 4, the header information and the format of the event dates are displayed following the website of EM-DAT.

Table 3. Identification and characterization of wet-related events (adapted from EM-DAT disaster database, accessed in 03-2021).

Dis No	Year	Disaster			Country	Affected regions (NUTS 2)	Dates		Figure
		Sub-group	Type	Subtype			Start	End	
1996-0006-PRT	1996	H	Flood	Flash flood	PRT	Norte, Centro	1996-01-08	1996-01-08	4(a)
2000-0699-ESP	2000	H	Flood	Flash flood	ESP	Cataluña; Aragón, Castilla-La Mancha, Región de Murcia, Comunidad Valenciana	2000-10-20	2000-10-26	4(b)
2000-0814-ESP		M	Storm		ESP	Cantabria, Galicia, Principado de Asturias, Castilla y León	2000-12-5	2000-12-5	
2000-0813-PRT					PRT	Norte, Centro, Área Metropolitana de Lisboa, Alentejo, Algarve	2000-12-6	2000-12-6	
2000-0837-ESP					ESP	Cataluña, Aragón, Comunidad Valenciana	2000-12-29	2000-12-29	
2001-0040-PRT	2001	H	Flood	Riverine flood	PRT	Vila Real and Guarda provinces	2001-01-26	2001-01-29	
2004-0145-ESP	2004	H	Flood	Riverine flood	ESP	Andalucía	2004-03-27	2004-03-28	5(g)

Preprints (www.preprints.org) | NOT PEER-REVIEWED | Posted: 21 April 2021 doi:10.20944/preprints202104.0577.v1

2010-0088-ESP	2010	M	Storm	extratropical storm Xynthia	ESP	Galicia, Principado de Asturias, Cantabria, País Vasco, Castilla y León	2010-02-27	2010-02-28	4(c)
2010-0088-PRT					PRT	Norte	2010-02-27	2010-02-27	
2018-0361-ESP	2018	H	Flood		ESP	Cataluña, Andalucía	2018-10-9	2018-10-11	4(d)
2019-0626-ESP	2019	M	Storm	extratropical storm Elsa/Fabien	ESP	Cataluña	2019-12-19	2019-12-22	4(e), (f)
2019-0626-PRT					PRT	Norte, Centro, Área Metropolitana de Lisboa	2019-12-19	2019-12-22	

[1] In the table H - Hydrological, M - Meteorological, ESP - Spain, PT - Portugal.

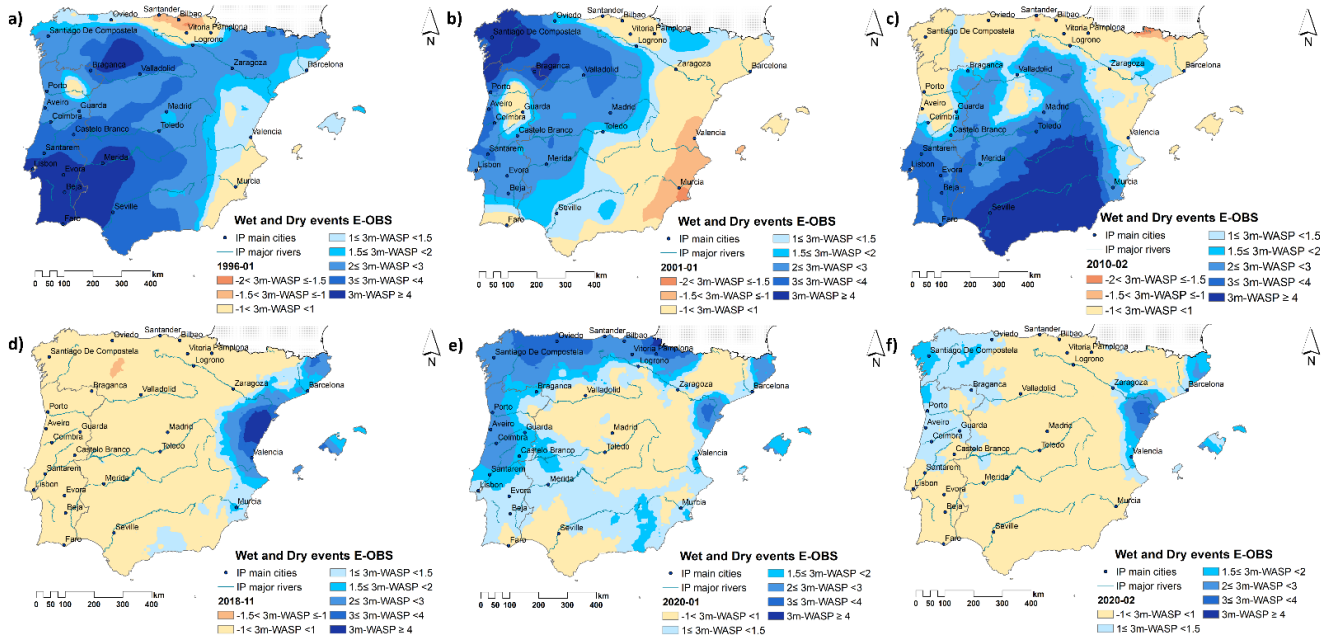

Figure 3. Spatial representation of wet events identified in the EM-DAT disaster database in Table 4 for (a) 3m-WASP 01-1996 (flood), (b) 3m-WASP 01-2001 (storm and flood), (c) 3m-WASP 02-2010 (extratropical storm Xynthia), (d) 3m-WASP 11-2018 (flood and Tropical cyclone Leslie), (e) 3m-WASP 01 2020 (extratropical storms Elsa and Fabien), (f) 3m-WASP (extratropical storms Elsa and Fabien).

Figure 3a represents the 3m-WASP January 1996 flood event, highlighting the beginning of a widespread severe wet event. The EM-DAT characterizes these events as flash floods. The WASP-index reaches values above 3, being most of the IP affected, except for Murcia, Cantabria, and País Vasco regions. According to EM-DAT (Table 3), the most affected regions are the Centro and Norte regions (in Portugal), as is corroborated by the WASP-index. However, since the WASP-Index in this study is calculated on a 3-, 6- and 12-monthly basis, these short-duration events, like flash floods, are not fully captured. Although the event is depicted, not always the most affected region described in EM-DAT corresponds to the spatial distribution shown in Figure 3. Despite this limitation, several wet events can still be identified by the 3m-WASP.

Table 4. Identification and characterization of dry-related events (adapted from EM-DAT disaster database, accessed in 03-2021).

Preprints (www.preprints.org) | NOT PEER-REVIEWED | Posted: 21 April 2021 doi:10.20944/preprints202104.0577.v1

Dis No	Year	Disaster			Country	Location	Dates		Figure
		Sub-group	Type	Subtype			Start	End	
1980-9359-ESP	1980	C	Drought	Drought	ESP	Southern region	1980	1983	5(a), (b)
1981-9130-ESP	1981						1981	1981	
1985-0096-ESP	1985	C	Wildfire	Land fire (brush, bush, pasture)	ESP	Comunidad Valenciana, Castilla y León, Castilla-La Mancha, Comunidad de Madrid	1985-08-06	1985-08-06	5(c)
1985-0271-ESP				Forest fire		Galícia, Andalucía	1985-09-12	1985-09-12	
1997-9105-PRT	1997	C	Drought	Drought	PRT		1997-04	1997	5(f)
2004-0383-PRT	2004	C	Wildfire	Forest fire	PRT	Norte, Centro and Faro	2004-07	2004-08	5(g), (h)
2004-9704-PRT			Drought	Drought		All provinces selected	2004-09	2005	
2005-0380-ESP	2005	C	Wildfire	Forest fire	ESP	Castilla-La Mancha	2005-07-18	2005-07-18	5(i)
2017-0417-PRT	2017	C	Wildfire	Forest fire	PRT	Centro	2017-10-15	2017-10-16	5(j), (k)
2017-0417-ESP					ESP	Galicia, Principado de Asturias	2017-10-17	2017-10-17	

[2] C - Climatological, ESP - Spain, PT - Portugal.

In 2000, Figure 3b shows a severe wet event in January 2001 3m-WASP that comprises the entire Portuguese territory (severe floods have occurred in the Mondego River basin), but also in Andalucía, Extremadura, Castilla-La Mancha, Comunidad de Madrid, Castilla y León and Galicia regions. The results are supported by the EM-DAT disaster database (Table 3), which identifies a sequence of several storms and flood events from October 2000 to January 2001. The latter events (October 2000 to January 2001) have affected the areas identified in Figure 3b.

In 2010, Figure 3c shows the February 2010 3m-WASP wet event, which affected central and southern areas of IP, and shows the path of the extratropical storm Xynthia across the Norte and Castilla y León regions, as also referred to in EM-DAT (Table 3).

The November 2018 (Figure 3d) and December 2018 3m-WASPs wet events reflect the flood event in Cataluña and Andalucía regions in October 2018, also registered in EM-DAT (Table 3).

According to EM-DAT, at the end of 2019 and the beginning of 2020, a sequence of extratropical storms stroke mainland Portugal (Table 3). Figures 3e and 3f show the spatial distribution of January 2020 3m-WASP, a footprint of the extratropical storms Elsa and Fabien. The most affected areas were Cataluña, Norte, and Centro (Table 3).

The aforementioned limitations regarding the identification of short-duration wet events are less noticeable for intermediate-to-severe dry events, as these events tend to be much more persistent in time. Therefore, they tend to be reliably captured, in both time and space, by the three timescales of the WASP-indices, depending on their severity and

Preprints (www.preprints.org) | NOT PEER-REVIEWED | Posted: 21 April 2021 doi:10.20944/preprints202104.0577.v1

duration. As for the wet events, a few examples described in Table 4 are described herein (Figure 4).

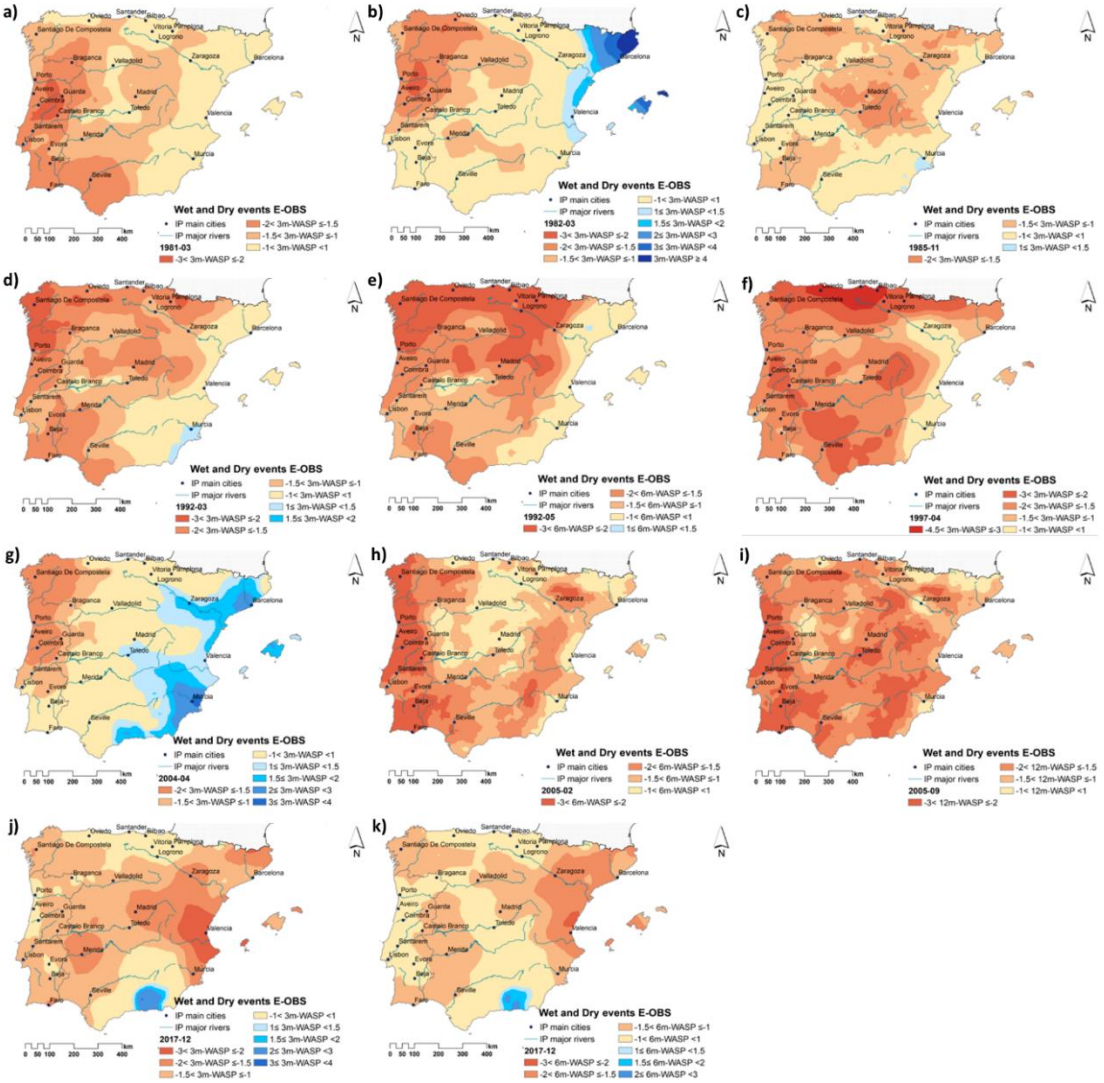

Figure 4. Spatial representation of dry events identified in the EM-DAT disaster database in Table 5 and [32] for (a) 3m-WASP 03-1981 (drought), (b) 3m-WASP 03-1982 [32], (c) 3m-WASP 11-1985 (wildfire), (d) 3m-WASP 03-1992 [32], (e) 6m-WASP 05-1992 [32], (f) 3m-WASP 04-1997 (drought), (g) 3m-WASP 04-2004 (flood and drought), (h) 6m-WASP 02-2005 ([32]; wildfire, heatwave; ECA), (i) 12m-WASP 11-2005 ([32]; wildfire), (j) 3m-WASP 12-2017 (wildfire, drought), (k) 6m-WASP 12-2017 (wildfire, drought).

The March 1981 3m-WASP (Figure 4a) reveals a moderate/intermediate dry event in most of the IP, except for the easternmost region, País Vasco, and Comunidad Foral de Navarra. In the Centro region (Portugal), this event was severely dry, with WASP values decreasing below –2. According to EM-DAT (Table 4), the Spanish southern region was under a drought from 1980 to 1983, and this drought was extended throughout the IP in 1981.

In 1982, a severe dry event is shown in March 1982 3m-WASP (Figure 4b) in Galicia and Asturias. The 3m-WASP values rise above –3, hinting at a severe dry event. This event also reaches other regions, such as Extremadura, Castilla y León, and Portugal. This result is in agreement with the results obtained by [32], including the wet area in Cataluña and Comunidad Valenciana, also detected here.

Preprints (www.preprints.org) | NOT PEER-REVIEWED | Posted: 21 April 2021 doi:10.20944/preprints202104.0577.v1

Figure 4c shows November 1985 3m-WASP and highlights persistent dry conditions in Comunidad Valenciana, Comunidad de Madrid, Castilla-La Mancha, Castilla y León, Galícia, and Andalucía, which may have driven the wildfires between August and September of 1985 reported by EM-DAT (Table 4).

In 1992, for March 3m-WASP and May 6m-WASP (Figures 4d and 4e), a severe dry event in Norte (Portugal) and Galicia is shown for the first index, then spreading to Asturias, Cantabria, País Vasco, Comunidad Foral de Navarra and Aragón in the second index (Figure 4e). In Figure 4d, an intermediate wet event in Región de Murcia is also detected. These results are also in accordance with [32], except for the wet event in Cataluña, which is identified here.

Figure 4f shows 3m-WASP for April 1997, corresponding to a severe dry event, with WASP values between −3 and −4.5. This event has affected most of the territory, with the exception of Región de Murcia, Comunidad Valenciana and Aragón. According to EM-DAT (Table 4), this severe dry event has strongly affected Portugal, which is also detected by this analysis.

Table 5. Number of intermediate-to-severe wet and dry events for the past periods 1961−1990, 1981−2010, and for the future periods 2021−2050 and 2041−2070, under RCP4.5 and RCP8.5.

Wet events		**1961−1990**	**1981−2010**	**2021−2050**		**2041−2070**	
				RCP4.5	**RCP8.5**	**RCP4.5**	**RCP8.5**
12m-WASP	**IW**	2	0	2	0	2	0
	SW	1	0	0	0	0	0
6m-WASP	**IW**	9	4	3	3	6	2
	SW	0	0	4	0	4	0
3m-WASP	**IW**	7	6	4	5	3	10
	SW	3	4	6	1	6	4
Dry events							
12m-WASP	**ID**	1	10	8	18	14	23
	SD	0	0	10	4	8	2
6m-WASP	**ID**	0	13	12	8	14	11
	SD	0	1	4	4	3	0
3m-WASP	**ID**	3	13	7	11	9	9
	SD	0	0	2	1	3	0

[3] In the table ID – Intermediately dry, IW – Intermediately wet, SD – Severely dry, SW – Severely wet.

In 2004, the April 2004 3m-WASP (Figure 4g) shows a severe wet event in Cataluña, Comunidad Valenciana, Aragón, Castilla-La Mancha, Región de Murcia, and Andalucía. From EM-DAT, a flood event was registered in Andalucía (Table 3). It is also detected an intermediate dry event in Alentejo, Área Metropolitana de Lisboa, Centro, Norte (in Portugal) and in Galicia and Castilla y León (in Spain), which is in agreement with the IPMA Climatological Report that considered 2004 a very dry year in Portugal [53,54]. Despite not registered in this database, the IPMA Climatological Report refers to December 2003 as a wet month, as well as a higher-than-average precipitation record on 30 January 2004 in Área Metropolitana de Lisboa.

In 2005, [32] have detected a severe wet event in February 2005 3m-WASP in the Murcia region, and a severe dry event in western Iberia (Portugal and Galicia). The European Climate Assessment & Dataset Extreme Events dataset also refers to this event in the IP as a heat and drought episode in Southern Europe (Summer 2005). These dry events are indeed detected by February 2005 6m-WASP (Figure 4j) and November 2005 12m-WASP (Figure 4k).

Preprints (www.preprints.org) | NOT PEER-REVIEWED | Posted: 21 April 2021 doi:10.20944/preprints202104.0577.v1

In 2017, the December 2017 3m-WASP (Figure 4j) and December 2017 6m-WASP (Figure 4k) show persistent dry conditions that can help to explain the devastating October 2017 wildfires in central Portugal (Table 4).

3.2. Historical trends and projections for wet and dry events

3.2.1. Historical trends for wet and dry events

The analysis of 12m-WASP, 6m-WASP, and 3m-WASP values in both Table 5 and Figure 5 (only for the past periods), will allow a better understanding of past and future conditions for dry and wet events for the entire IP, under RCP4.5 and RCP8.5. According to Table 5, a single 12m-WASP intermediate dry (ID) event and three 3m-WASP ID events were detected for the study area in the period 1961–1990 (Figure 5). No severe dry (SD) events were detected. For 3m-WASP, 7 intermediate wet (IW) and 3 severe wet (SW) events are shown for the same period, 9 IW and no SW for 6m-WASP, and 2 IW and one SW for 12m-WASP (Figure 5).

For 1981–2010 no SW events were detected, except for 3m-WASP, with 4 SW events. Similar considerations can be made for the SD events, apart from 1 event for 6m-WASP. For this period, 4 IW events were detected for 6m-WASP and 6 for 3m-WASP. Conversely, in 1981–2010, 10 ID events are found for 12m-WASP, 13 ID events for 6m- and 3m-WASP, hinting at an upward trend in dry conditions (Figure 5).

The results project an increase in the number of both intermediate-to-severe dry events, between 2021–2050 and 2041–2070, under both RCPs, and for the three WASP timescales. The number of projected events is higher than for the intermediate-to-severe wet events. A higher number of dry events are projected, with 12m-WASP higher for RCP8.5 (23 ID and 2 SD) than for RCP4.5 (14 ID and 8 SD) over the period 2041–2070 (Table 5). The increase of the intermediate-to-severe wet events is not as pronounced as for the dry events (Table 5), for both 12m-WASP (Figure 5a) and 6m-WASP (Figure 5b).

Preprints (www.preprints.org) | NOT PEER-REVIEWED | Posted: 21 April 2021 doi:10.20944/preprints202104.0577.v1

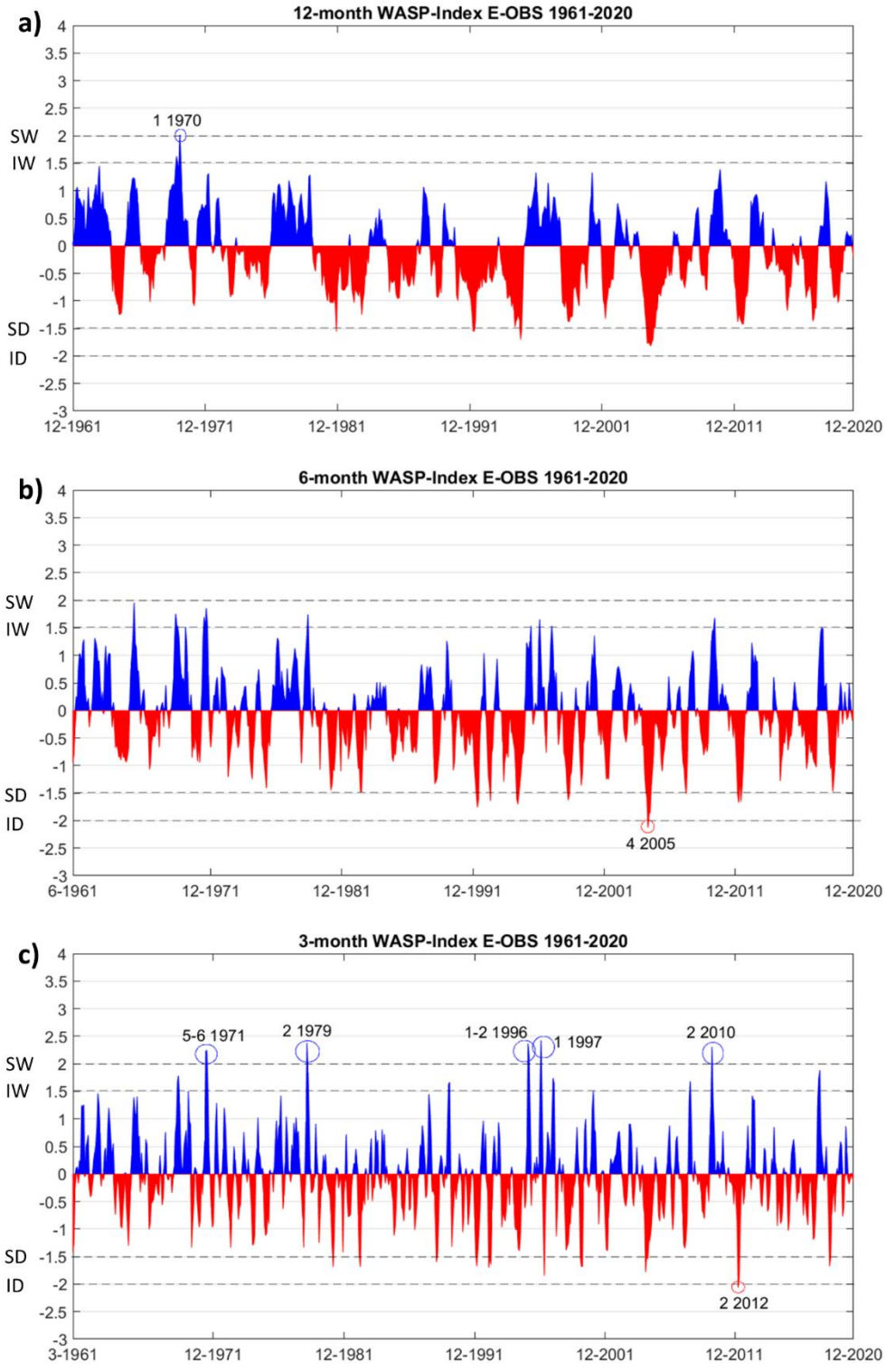

Figure 5. Mean areolar values between 1961–2070 for a) 12m-WASP, b) 6m-WASP and c) 3m-WASP-Index in which intermediate-to-severe dry (red) and wet (blue) events are identified (months year).

As mentioned in section 3.1., wet events are typically associated with shorter time-scales (e.g., flash floods, floods, and storms). Therefore, they are better captured with the smaller timescale WASP-Index. For the 3m-WASP in 2041–2070, 10 IW and 4 SW events were found under RCP8.5, and 3 IW and 6 SW under RCP4.5. These results hint at a link between drought conditions and extreme climatological events (higher values in 12m-WASP) and wet conditions and extreme meteorological events (higher values in 3m-

Preprints (www.preprints.org) | NOT PEER-REVIEWED | Posted: 21 April 2021 doi:10.20944/preprints202104.0577.v1

WASP). The projections for the number of SW events for 3m-WASP (6 and 1 for 2021–2050, 6 and 4 for 2041–2070, for RCP4.5 and RCP8.5, respectively) is higher in comparison with the SD events (2 and 1 for 2021–2050, 3 and 0 for 2041–2070, for RCP4.5 and RCP8.5, respectively) (Table 5). No intermediate-to-severe wet events are projected to occur for the 12m-WASP under RCP8.5. Only 2 IW events are projected for both future periods under RCP4.5.

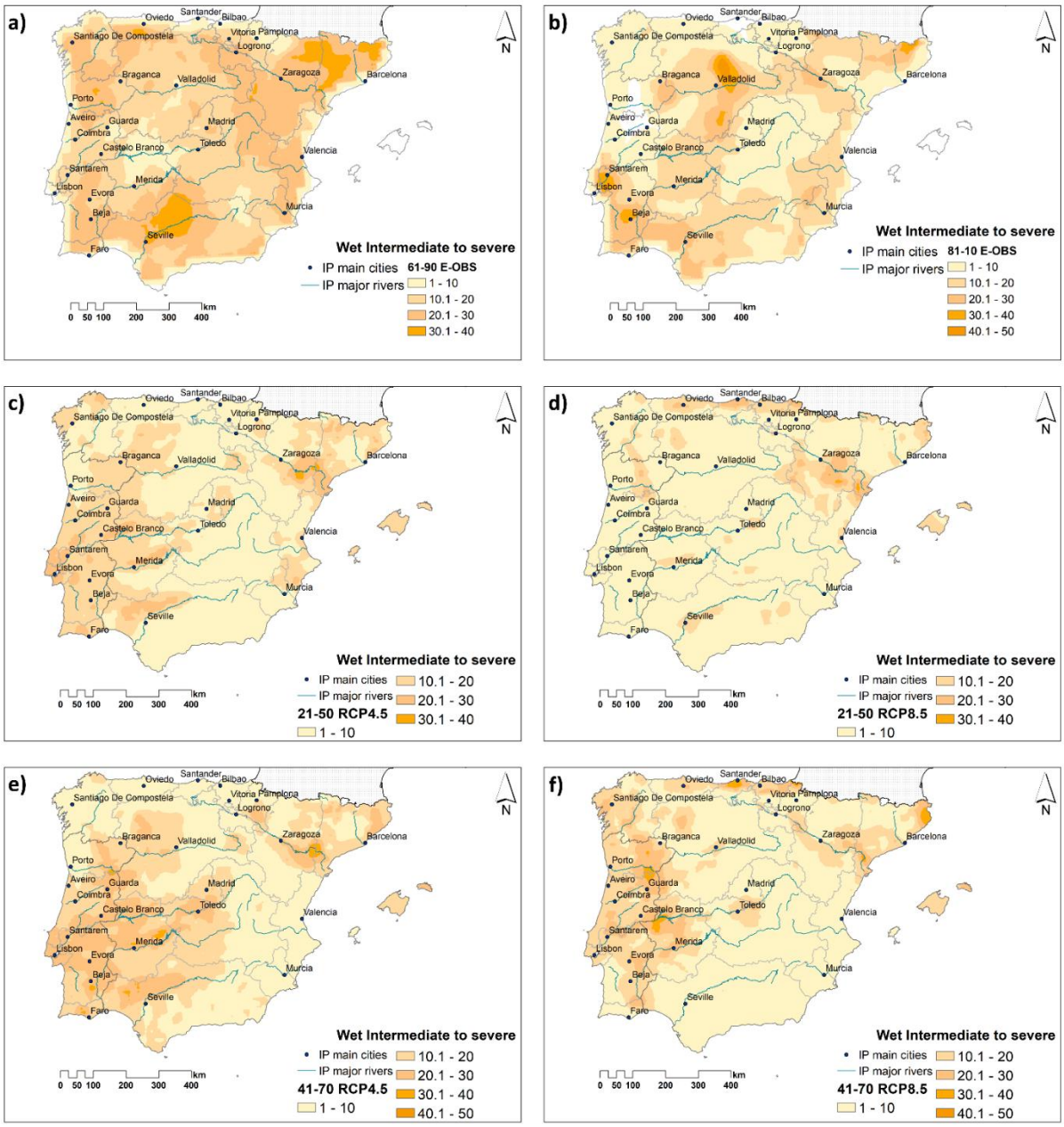

Figure 6. Duration in months of 12m-WASP intermediate-to-severe wet events in IP for the periods a) 1961–1990, b) and c) 1981–2010, d) and e) 2021–2050, f) and g) 2041–2070, under RCP4.5 (left) and RCP8.5 (right) (Note: NUTS 2 in grey contours).

Preprints (www.preprints.org) | NOT PEER-REVIEWED | Posted: 21 April 2021 doi:10.20944/preprints202104.0577.v1

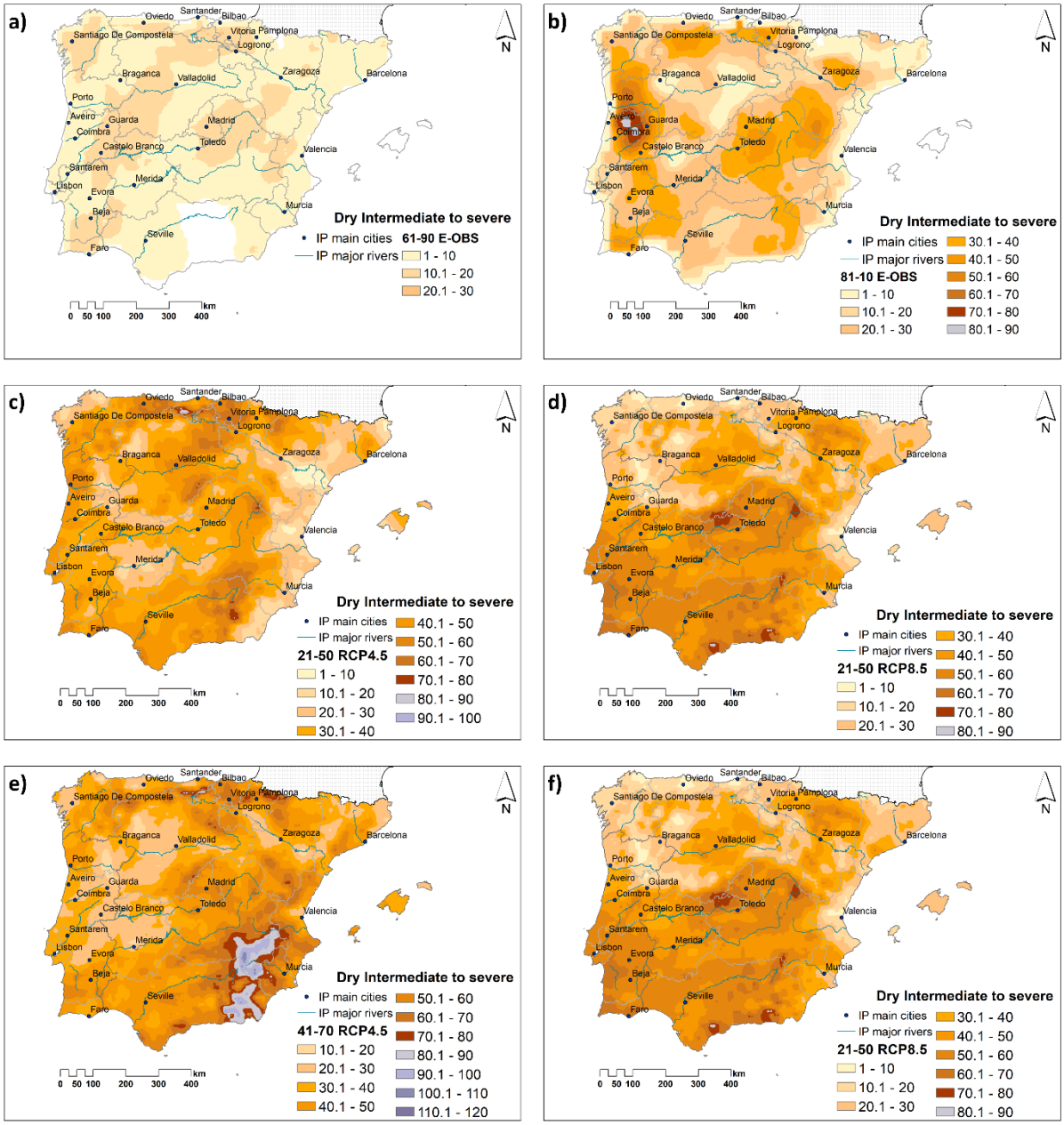

Figure 7. Duration in months of 12m-WASP intermediate-to-severe dry events in IP for the periods a) 1961–1990, b) and c) 1981–2010, d) and e) 2021–2050, f) and g) 2041–2070, under RCP4.5 (left) and RCP8.5 (right) (Note: NUTS 2 in grey contours).

In summary, an overall increase of ID events is projected, more pronounced than for the SD events, and higher for 12m-WASP under RCP8.5 (Table 5). For 6m-WASP, the projected number of dry events is also noticeable, also higher for ID (12 and 8 for 2021–2050, 14 and 11 for 2041–2070, for both RCPs, respectively) than for SD events (4 and 4 for 2021–2050, 3 and 0 for 2041–2070, for both RCPs, respectively). As stated above, the projected increase of intermediate-to-severe wet events is not as pronounced as for dry events. The 3m-WASP IW events show the most significant change under RCP8.5 (4 and 5 for 2021–2050, 3 and 10 for 2041–2070, for both RCPs, respectively). For 12m-WASP, no significant increase in the number of IW events is projected under RCP4.5, for which no SW events are projected to occur from 2021 to 2070 under both RCPs.

Following the selected methodology (Figure 2), the duration (Figures 6 and 7), intensity (Figures 9 and 10), and frequency of occurrence (Figures 11 and 12) for intermediate-

Preprints (www.preprints.org) | NOT PEER-REVIEWED | Posted: 21 April 2021 doi:10.20944/preprints202104.0577.v1

to-severe wet and dry events for 12m-WASP were computed for the past periods 1961–1990 and 1981–2010, and the future periods 2021–2050 and 2041–2070, under RCP4.5 and RCP8.5. The 12m-WASP anomalies (**Δ**) between 2041–2070, for both RCPs, and 1961–1990 are presented for the duration (Figure 8) and frequency of occurrence (Figure 13) of wet and dry events. The corresponding tables for intensity (Table S1), duration (Table S2), and frequency (Table S3) were analyzed for several IP main cities (within NUTS 2 regions) and are provided as supplementary material.

3.2.2. Projections for wet and dry events

Figure 6 shows the duration in months of intermediate-to-severe wet events for 12m-WASP under both RCPs. The results show a clear projected decrease in the duration of these events from 1961–1990 (Figure 6a) to 1981–2010 (Figure 6b) in Aragón and Cataluña, despite the increase in the duration over central Iberia and southern Portugal. This hints at a change in the precipitation regime during these periods. Conversely, for the same periods, there is an outstanding difference between the duration of intermediate-to-severe dry events in 1961–1990 (Figure 7a) and 1981–2010 (Figure 7b). An increase in the number of dry months in Centro, Norte (in Portugal), and Galicia are noteworthy, with values reaching 90 months (corresponding to 7.5 years) for 1981–2010 (Figure 7a). The high number of intermediate-to-severe dry months (30 to 70 months; 2.5 to 5.8 years) can also be found in the north, between Oviedo and Zaragoza, inner Iberia (surrounding Madrid, Toledo, Valencia, and Murcia), and in between Merida and Seville (Figure 7b).

A decrease in the number of intermediate-to-severe wet months is apparent, more pronounced for 2041–2070 (Figures 6e and f) than for 2021–2050 (Figures 6c and d), and lower under RCP8.5 (Figure 6f) than RCP4.5 (Figure 6e). This decrease is clear for 2041–2070 (Figures 8a and 8b), for which most of the IP shows negative anomalies under both RCPs. The region with higher duration is located near the Atlantic Ocean, over Portugal (positive anomalies), extending towards Extremadura in Spain, mainly under RCP4.5. This projected decrease in the duration can also be found in southern Portugal, affecting the Alentejo and Algarve regions in both periods, mainly under RCP8.5 and for 2021–2050. Conversely, the projected increase in the number of months of intermediate-to-severe dry events is worth noting (Figures 7c to f). The spatial extension of the highest values towards the southern half of IP is also clear, though for 2021–2050 there are areas with lower values in inner Iberia and the eastern coast, mainly under RCP4.5 (Figure 7c) when compared with RCP8.5 (Figure 4d). The highest durations (up to 120 months, e.g., equivalent to 10 years) are projected for the region of Murcia and its surroundings, with a more prominent extension under RCP4.5 (Figure 7e). Although the extension of these maximum values is weaker under RCP8.5, small areas in the north (between Oviedo and Vitoria, Logroño; Figure 7f) can also be identified for 2041–2070. The corresponding positive differences are shown in Figures 8c and 8d, with prominent values in the previously stated regions. Hence, for these areas, one-third of the years (approximately 10 years) in the period 2041–2070 will experience intermediate-to-severe dry conditions under both RCPs.

Preprints (www.preprints.org) | NOT PEER-REVIEWED | Posted: 21 April 2021 doi:10.20944/preprints202104.0577.v1

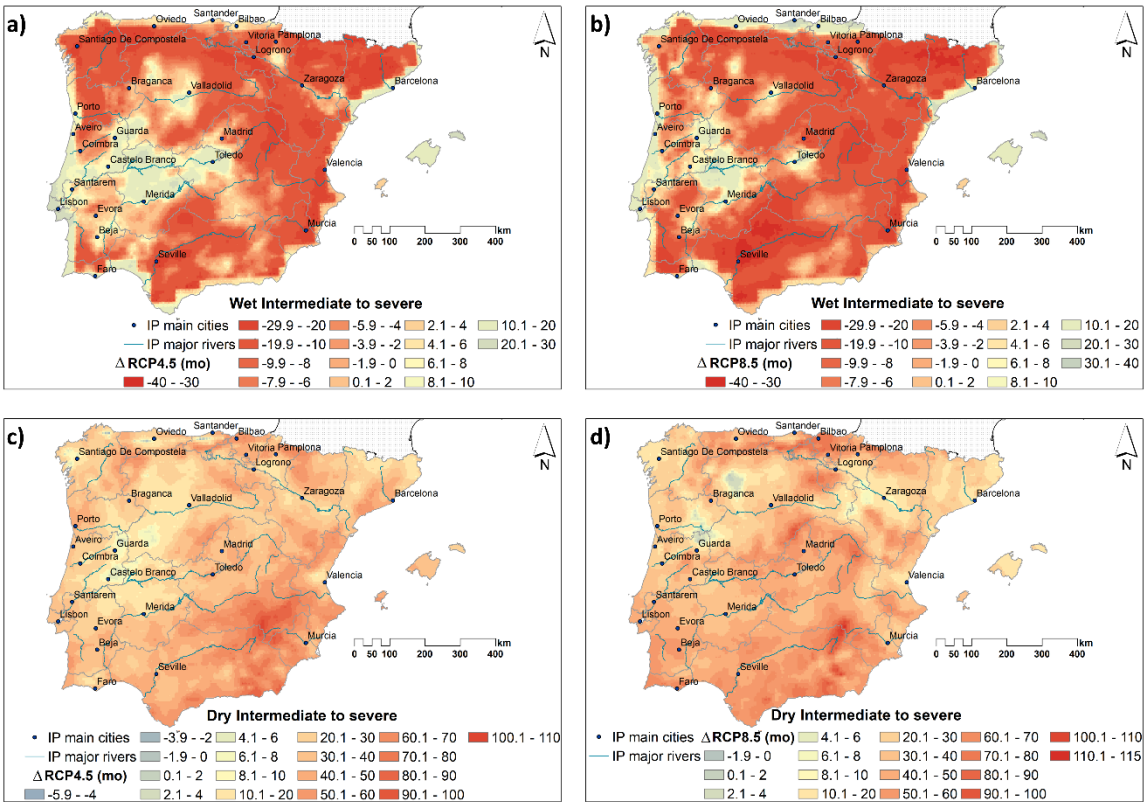

Figure 8. Differences between 2041–2070 and 1961–1990 for the duration, in months, of 12m-WASP intermediate-to-severe wet events in IP under a) RCP4.5 (left) and b) RCP8.5; and for the intermediate-to-severe dry events in IP under c) RCP4.5 (left) and d) RCP8.5. (Note: NUTS 2 in grey contours; and **Δ**(41–70 - 61–90)).

Figure 9 shows the spatial-temporal evolution of intermediate-to-severe wet events for the 12m-WASP past and future periods, under RCP4.5 and RCP8.5. Clear differences between the past and future periods are found. The extensions of areas with SW events (> 2) for 1961–1990 decrease for 1981–2010 (though Galicia presents values >2.6). However, for 2021–2050 and both RCPs, the prominence of IW events through the southeast of Iberia is apparent. This predicted decrease of intensity of SW areas in most of IP is higher between 2041–2070, mainly for RCP8.5 (Figure 9f). Although an intensity decrease is found for severe events under RCP8.5, an area comprising most of the Portuguese territory, western Andalucía, Extremadura, certain regions of Castilla y Léon and Cataluña remain with conditions favorable to the occurrence of SW conditions towards 2070 and under RCP4.5 (Figure 9g).

Preprints (www.preprints.org) | NOT PEER-REVIEWED | Posted: 21 April 2021 doi:10.20944/preprints202104.0577.v1

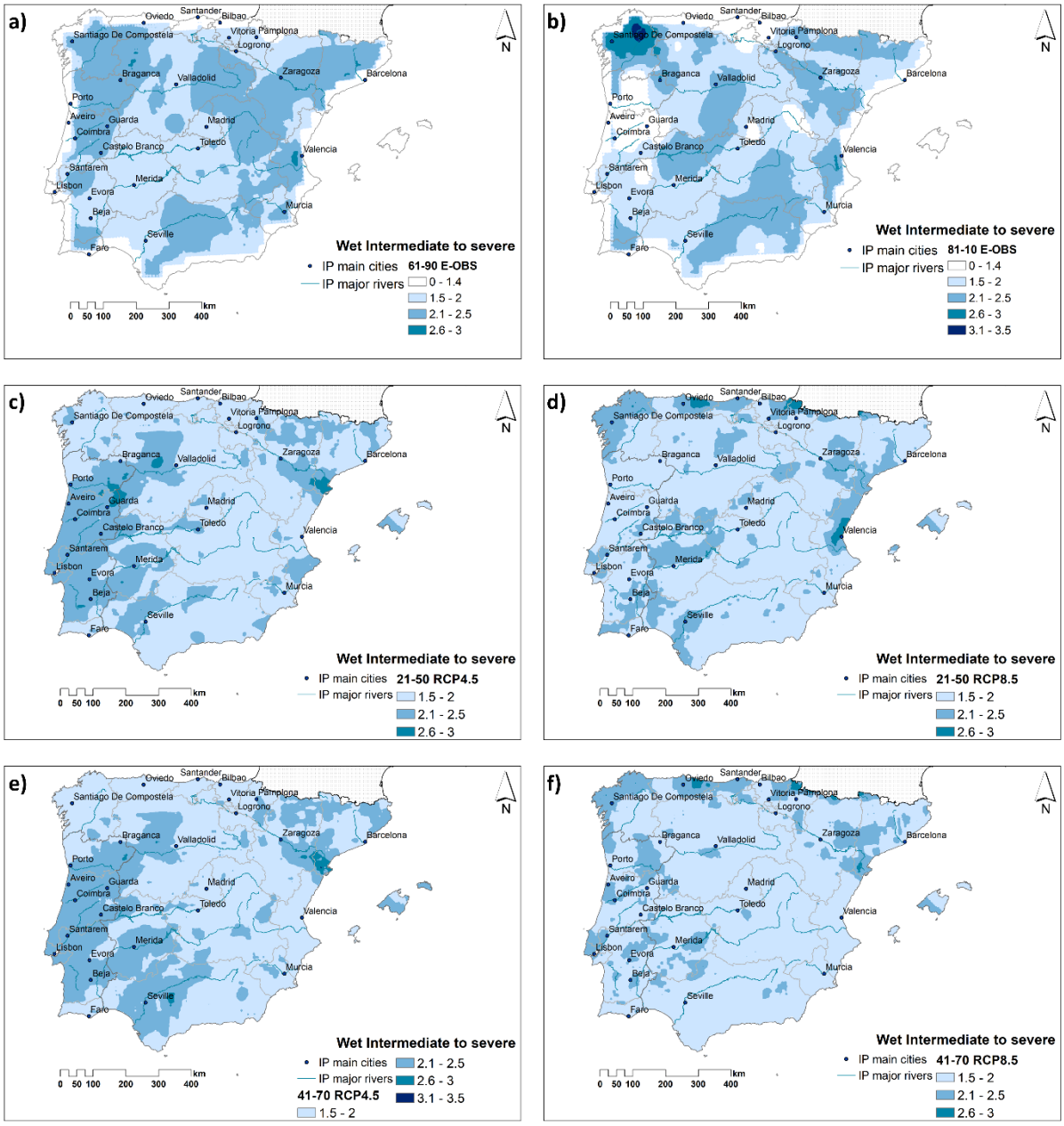

Figure 9. Intensity of 12m-WASP intermediate-to-severe wet events in IP for the periods a) 1961–1990, b) and c) 1981–2010, d) and e) 2021–2050, f) and g) 2041–2070, under RCP4.5 (left) and RCP8.5 (right) (Note: NUTS 2 in grey contours).

Although ID conditions prevailed over the two past periods (Figures 10a and c) in the westernmost half of the IP from 2021 onwards (Figure 10a to c), most of the territory may experience SD conditions, mainly for RCP4.5 and 2041–2070 (Figure 10e). Similar results are found for RCP8.5, projecting areas of ID conditions in Galicia, Castilla y Léon, Aragón, and Valencia, in Spain, and Centro and Norte, in Portugal (Figures 10d and f).

Preprints (www.preprints.org) | NOT PEER-REVIEWED | Posted: 21 April 2021 doi:10.20944/preprints202104.0577.v1

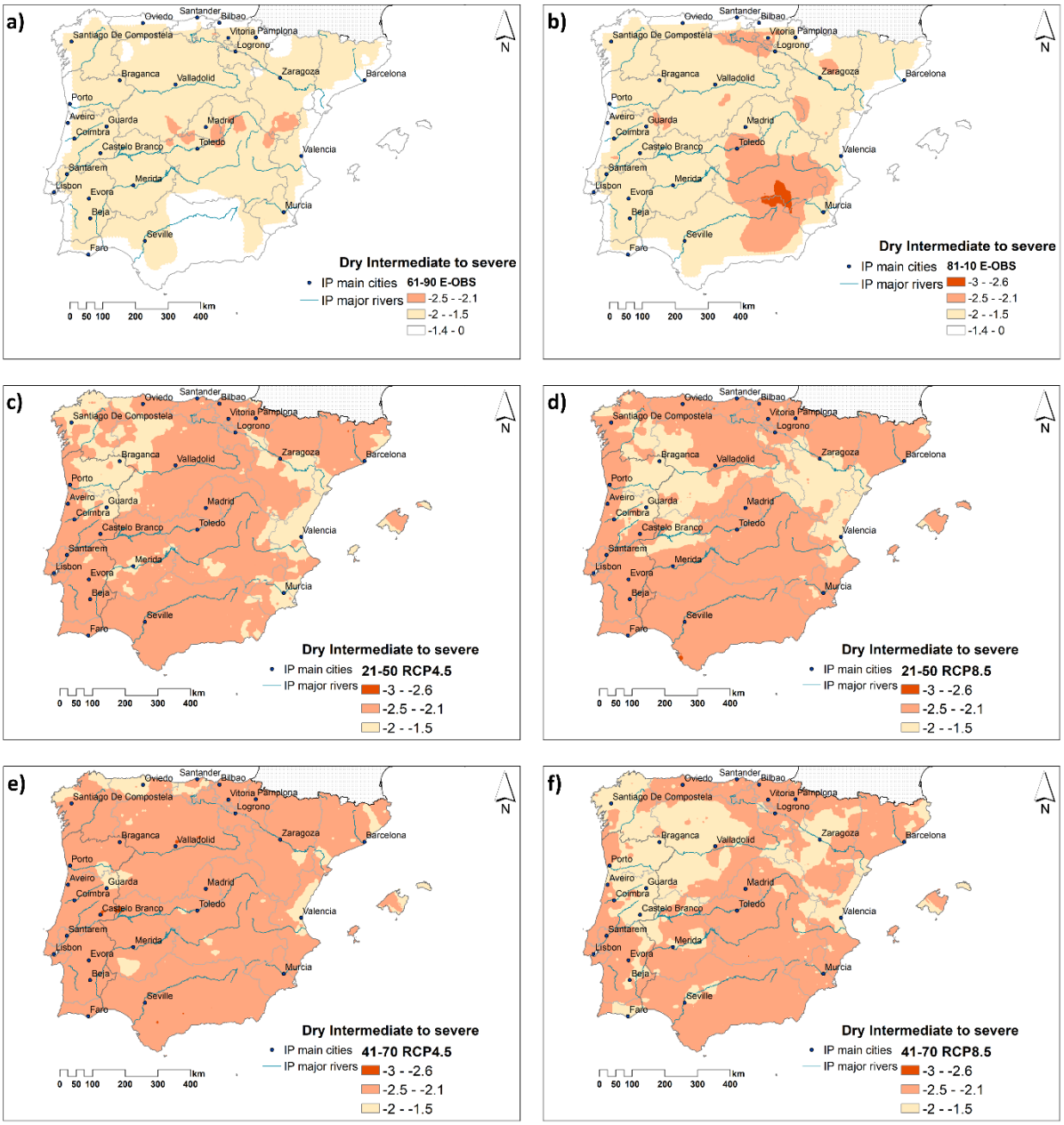

Figure 10. Intensity of 12m-WASP intermediate-to-severe dry events in IP for the periods a) 1961–1990, b) and c) 1981–2010, d) and e) 2021–2050, f) and g) 2041–2070, under RCP4.5 (left) and RCP8.5 (right) (Note: NUTS 2 in grey contours).

Figure 11 shows the frequency of occurrence of intermediate-to-severe wet events that reveals an overall decrease of these events from 2021–2050 under RCP8.5 (Figure 11e) when comparing with the past periods (Figures 11a and b), as well as for the same period under RCP4.5 (Figure 11d). The period 2041–2070 reveals higher probabilities of occurrence of wet events in the westernmost part of the IP (Galicia not included under RCP4.5) and in the vicinity of Zaragoza and Barcelona (Aragon and Cataluña provinces) (Figures 11e and f), though with lower percentages under RCP8.5. For all periods, these percentages do not exceed 15%. A closer inspection of the spatial patterns between the past (Figures 11a and b) and future periods reveals contrasting differences (Figures 11c to f). These contrasting differences are also present for the frequency of occurrence of intermediate-to-dry events, but it is predicted an increase that might reach a maximum of 35% from 2021 until 2070 under both RCPs (Figure 12). The aforementioned decrease in the frequency is shown in the spatial representation of the anomalies for 2041–2070, in which the

Preprints (www.preprints.org) | NOT PEER-REVIEWED | Posted: 21 April 2021 doi:10.20944/preprints202104.0577.v1

negative signal is prominent, except for small areas in the Portuguese and northern Spanish coastal areas, as well as central Iberia in the vicinity of Murcia (positive anomalies), with higher expression under RCP8.5 (Figure 13a and b).

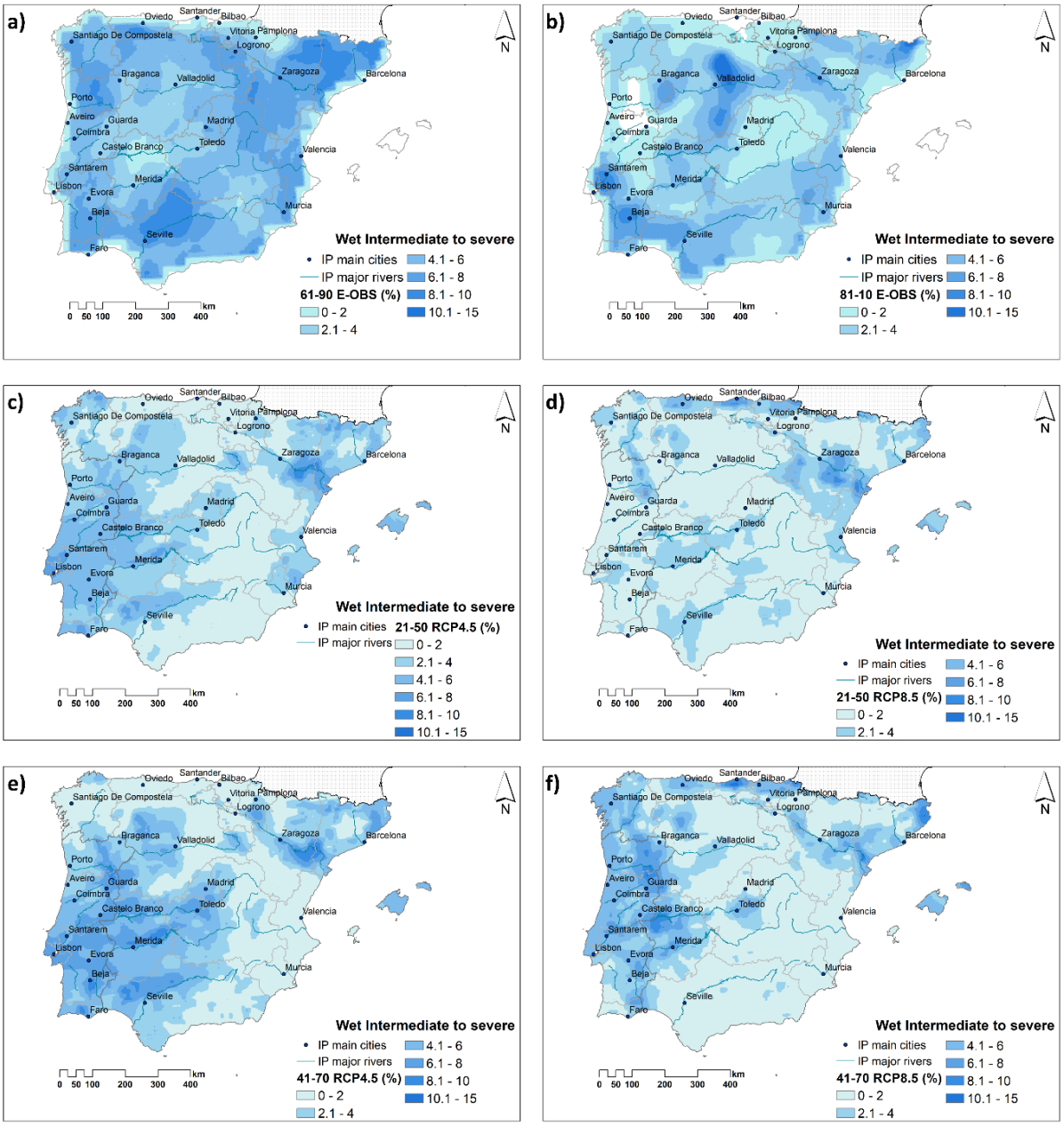

Figure 11. Probability (in %) of 12m-WASP intermediate-to-severe wet events in IP for the periods a) 1961–1990, b) and c) 1981–2010, d) and e) 2021–2050, f) and g) 2041–2070, under RCP4.5 (left) and RCP8.5 (right) (Note: NUTS 2 in grey contours).

Smaller frequencies of occurrence of intermediate-to-severe dry events up to 8% were recorded for 1961–1990 (Figure 12a), with areas with near-normal classification. However, clear changes can be observed for 1981–2010 (Figure 12b), in which the percentages of occurrence of dry events increased by nearly 25%, mainly in the Centro Region of Portugal. Projections show that for 2021–2050 the southern half of the IP (Comunidad de Madrid, Castilla-La Mancha, and Comunidad Valenciana, in Spain, and Centro, in Portugal) will be the most affected under RCP8.5 (Figure 12d). This includes the southern region of

Preprints (www.preprints.org) | NOT PEER-REVIEWED | Posted: 21 April 2021 doi:10.20944/preprints202104.0577.v1

Portugal (Algarve, Alentejo, and Área Metropolitana de Lisboa) that can reach 20% of intermediate-to-dry events under RCP8.5. For the same period (2021–2050) a broader belt from eastern Andalucía to Principado de Asturias, Cantabria, País Vasco and La Rioja with higher percentages are projected under RCP4.5 (Figure 12c). Projections show that the percentage of these dry conditions can reach 35% in certain regions of the IP, such as its central and south-eastern areas under both RCPs (Figures 12e and f). Southern Portugal also presents higher percentages, mainly under RCP8.5, with projected frequencies from 10 to 25%.

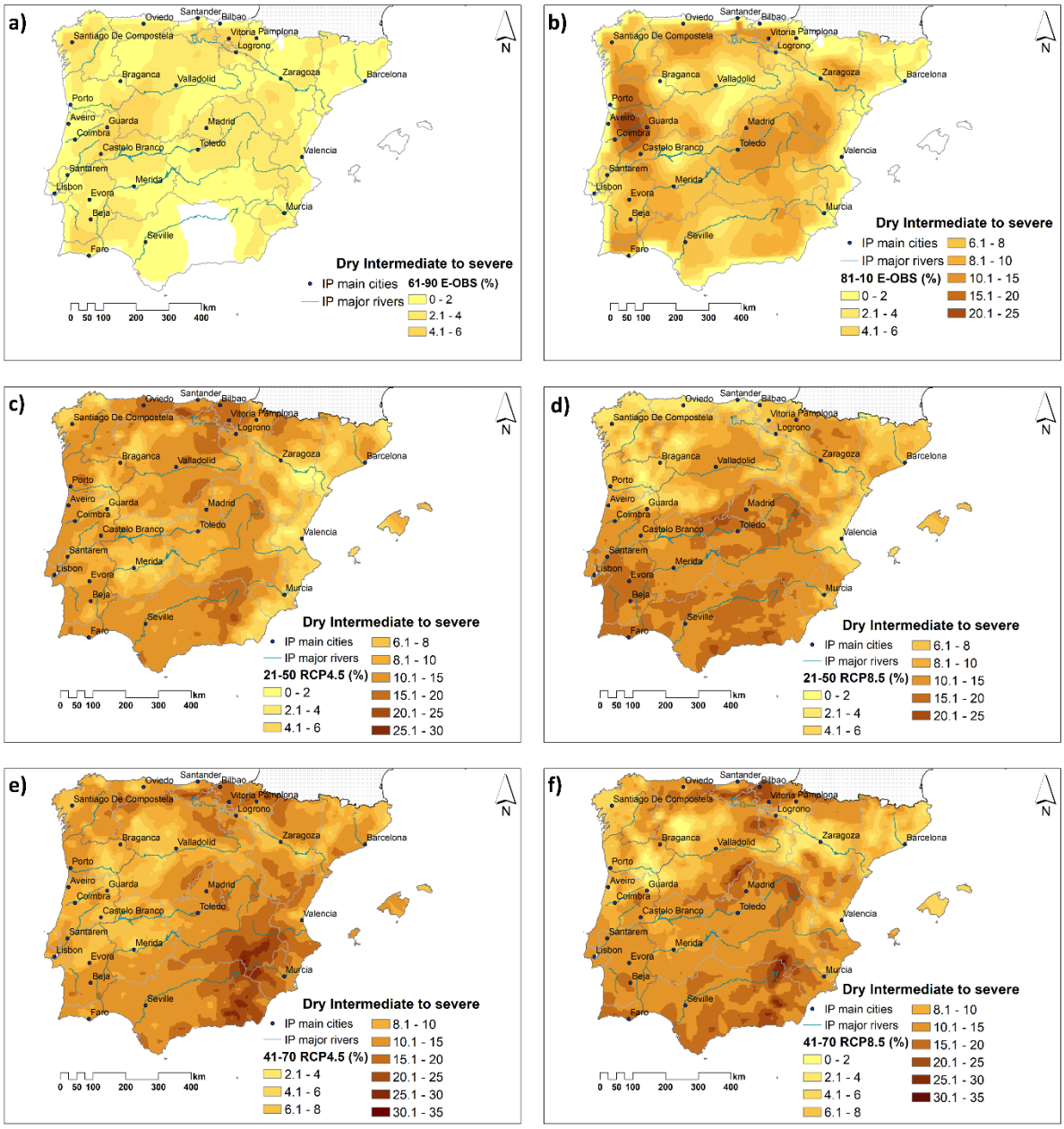

Figure 12. Probability (in %) of 12m-WASP intermediate-to-severe dry events in IP for the periods a) 1961–1990, b) and c) 1981–2010, d) and e) 2021–2050, f) and g) 2041–2070, under RCP4.5 (left) and RCP8.5 (right) (Note: NUTS 2 in grey contours).

Preprints (www.preprints.org) | NOT PEER-REVIEWED | Posted: 21 April 2021 doi:10.20944/preprints202104.0577.v1

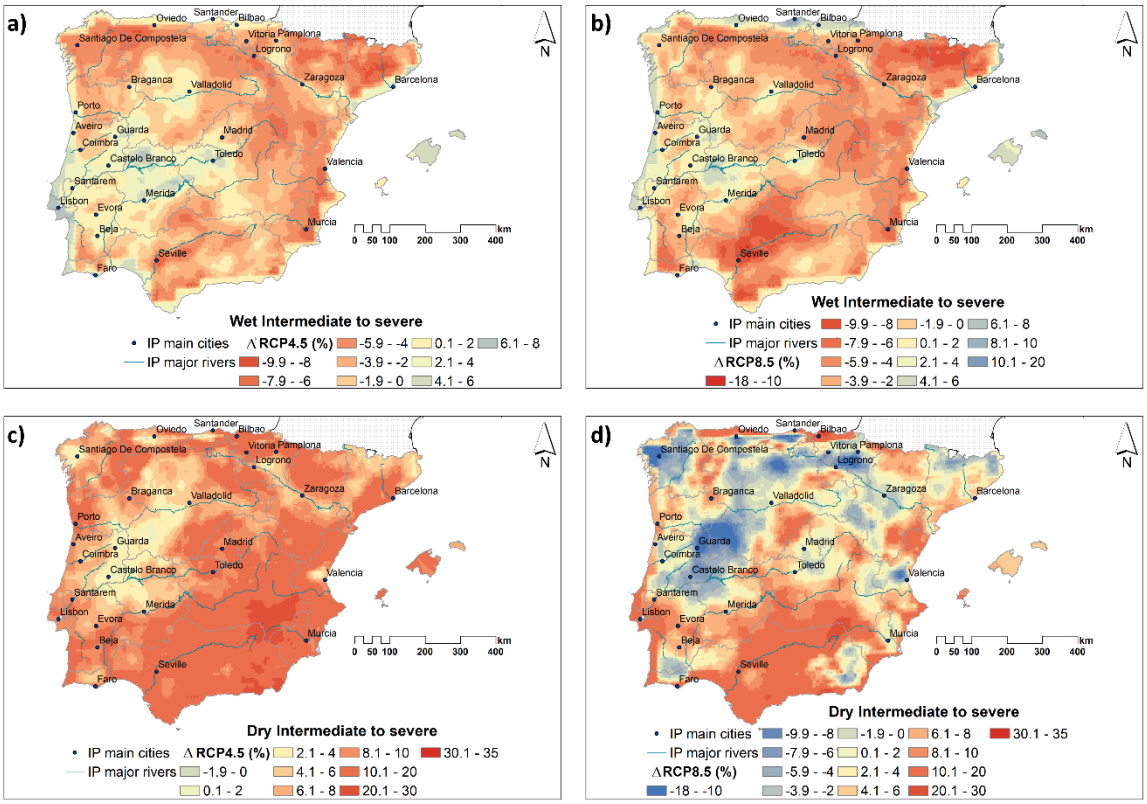

Figure 13. Differences between 2041–2070 and 1961–1990 for the frequency, in %, for the 12m-WASP intermediate-to-severe wet events in IP under a) RCP4.5 (left) and b) RCP8.5; and for the intermediate-to-severe dry events in IP under c) RCP4.5 (left) and d) RCP8.5 (Note: NUTS 2 in grey contours; and Δ(41–70 - 61–90)).

The analysis of the anomalies highlights the spatial variability of the frequencies of occurrence of the dry events towards 2070 (Figure 13c and d). While under RCP4.5 anomalies are positive through most of Iberia and up to 35% changes are projected, there are regions for which negative anomalies are found under RCP8.5 (Figure 13d), though smaller (up to –9.9%). This reveals how climate change projections will affect the IP in different ways, mainly regarding intermediate-to-severe dry events.

4. Discussion and Conclusions

In the present study, the ability of the WASP-index to capture extremely dry or wet events in the IP, registered in the EM-DAT disaster database and by a previous study by [32], was assessed over the period 1961–2020. This methodology assesses the performance of the WASP-Index in capturing wet and dry events in the IP, as most of the studies use the SPI or SPEI. Although most of these extreme events, particularly the meteorological or weather-driven events (e.g., floods or storms), typically occur in shorter timescales (hours to days), they have spatially coherent patterns with EM-DAT records and are still identified by the shorter monthly timescales of the WASP-index. For example, the 3m-WASP was able to capture the 2010 winter anomalous conditions [55]. This latter study analyzed the SPI for the IP and also refers that 1969 (also by [56]) and 1996 winters were very similar to 2010. Both winters are also captured by 3m-WASP (Figure 5c). These results show a reasonable performance of WASP-Index in capturing extreme wet events. However, the performance of 1m-WASP in detecting these wet events will be explored in future research. Conversely, for dry events, the three timescales of the WASP-Index were used. Conversely, for dry events, the three timescales of the WASP-Index were used. As an example, [57] used SPI at different timescales to construct a new global database of meteorological drought events from 1951 to 2016. For the IP, they have identified drought periods

between 1991–1995 and 2004–2007 that were also depicted by 3m-, 6m- and 12m-WASP (Figure 5). Overall, this analysis also enabled better documentation of some reported events, such as their intensity, duration, and spatial extension for the IP between 1961–2020. Furthermore, for this same period, the area-mean mean values over the IP revealed an upward trend in the frequency of occurrence of intermediate-to-severe dry events, which is in line with a general drying trend already reported by previous studies [2,4,23,32,51,58,59].

For the future climates, it was found an increase of the intensity, duration, and frequency of occurrence of the 12m-WASP intermediate-to-severe dry events under both RCPs, particularly in the southernmost regions of the IP. Indeed, these regions that comprise mainly Comunidad Valenciana, Región de Murcia, Andalucía (in Spain), Alentejo, and Algarve (in Portugal) will endure more prolonged and intense droughts until 2070, increasing the vulnerability of the ecosystems to water scarcity. The heterogeneity of the spatial patterns in the future, under both RCPs, also suggests changes in the large-scale patterns of daily precipitation in IP that were already identified in the past [60]. Furthermore, the upward trend in the dry events is projected to be strengthened in future climates, which is also in agreement with previous studies with related impacts on droughts [61], bioclimatic conditions [62], or climate classification [21,63]. Since droughts have deep impacts on water resources, agriculture, and the environment, this is particularly relevant. This standardized index and methodology can lead to the analysis of drought indices derived from the Standardized Soil Water Index (SSWI) [64]. In future research, the linkage of the agricultural Drought Hazard Index (DHI) with crop yields, can lead to the quantification of crop drought vulnerability and risks. This enables evaluating the water resources vulnerability and scarcity of this region. For instance, [38] evaluated water scarcity in the Middle East using the WASP-Index. Concerning the wet events, it is shown a decrease in the intensity, duration, and frequency of occurrence of the 12m-WASP intermediate-to-severe wet events. These outcomes are supported by previous research for the IP [55]. Nonetheless, the number of 3m-WASP intermediate-to-severe wet events is projected to increase, particularly for the severe events under RCP4.5, thereby suggesting a trend for a strengthening of shorter-term wet events and extreme precipitation episodes [16,65–68].

The assessment of wet and dry events is highly relevant in regions already considered climatic hotspots like the IP [18,20,69]. Drought risk analysis should be a primary concern of policymakers, as drought risk management should decrease the impacts of severe droughts in urban areas, in which water supply frequently depends on artificial storage. As an example, the Alqueva dam (Portugal) in the Guadiana river has a deep impact on the water supply for population and agriculture in Extremadura, Andalucía, and southern Portugal, for which the cities identified in this study (Supplementary material), like Faro (Tables S1, S2 and S3), are projected to endure more severe and prolonged dry conditions. Overall, this study allows concluding that there will be a greater propensity to the occurrence of dry events in the IP until 2070, under both RCPs, with inevitable consequences e.g. on ecosystems [37] or wildfire risk [24], also requiring changes in agricultural practices [9,70], such as a selection of new grapevine cultivars [71] or the implementation of olive tree irrigation [72].

Supplementary Materials: The following are available online at www.mdpi.com/xxx/s1, Tables S1, S2 and S3.

Author Contributions: For this study, the author's contribution was conceptualization, Andrade C; methodology, Andrade C and Santos J; software, Andrade C and Contente J.; validation, Andrade C and Santos JA; formal analysis, Andrade C; investigation, Andrade C; data curation, Contente J; writing—original draft preparation, Andrade C; writing—review and editing, Andrade C and Santos JA; visualization, Andrade C and Contente J; supervision, Santos JA. All authors have read and agree with the published version of the manuscript.

Funding: This research was funded by National Funds by FCT - Portuguese Foundation for Science and Technology, under the project **UIDB/04033/2020.** This study was funded by the European Commission-funded project "Climate change impact mitigation for European viticulture: knowledge transfer for an integrated approach – Clim4Vitis" [**grant 810176**].

Acknowledgments: We acknowledge the E-OBS dataset from the EU-FP6 project UERRA (https://www.uerra.eu) and the Copernicus Climate Change Service, and the data providers in the ECA&D project (https://www.ecad.eu).

References

1. Forzieri, G.; Feyen, L.; Russo, S.; Vousdoukas, M.; Alfieri, L.; Outten, S.; Migliavacca, M.; Bianchi, A.; Rojas, R.; Cid, A. Multi-Hazard Assessment in Europe under Climate Change. *Clim. Change* **2016**, *137*, 105–119, doi:10.1007/s10584-016-1661-x.
2. Viceto, C.; Cardoso Pereira, S.; Rocha, A. Climate Change Projections of Extreme Temperatures for the Iberian Peninsula. *Atmosphere* **2019**, *10*, 229, doi:10.3390/atmos10050229.
3. Portero Serrano, J.; Acero Díaz, F.J.; García García, J.A. Analysis of Extreme Temperature Events over the Iberian Peninsula during the 21st Century Using Dynamic Climate Projections Chosen Using Max-Stable Processes. *Atmosphere* **2020**, *11*, 506, doi:10.3390/atmos11050506.
4. Carvalho, D.; Cardoso Pereira, S.; Rocha, A. Future Surface Temperature Changes for the Iberian Peninsula According to EURO-CORDEX Climate Projections. *Clim. Dyn.* **2021**, *56*, 123–138, doi:10.1007/s00382-020-05472-3.
5. IPCC Climate Change 2013 – The Physical Science Basis: Working Group I Contribution to the Fifth Assessment Report of the Intergovernmental Panel on Climate Change Available online: https://www.cambridge.org/core/books/climate-change-2013-the-physical-science-basis/BE9453E500DEF3640B383BADDC332C3E (accessed on 14 April 2021).
6. Brown, C.; Meeks, R.; Hunu, K.; Yu, W. Hydroclimate Risk to Economic Growth in Sub-Saharan Africa. *Clim. Change* **2011**, *106*, 621–647, doi:10.1007/s10584-010-9956-9.
7. Brown, C.; Meeks, R.; Ghile, Y.; Hunu, K. Is Water Security Necessary? An Empirical Analysis of the Effects of Climate Hazards on National-Level Economic Growth. *Philos. Trans. R. Soc. Math. Phys. Eng. Sci.* **2013**, *371*, 20120416, doi:10.1098/rsta.2012.0416.
8. Holtermann, L. Precipitation Anomalies, Economic Production, and the Role of "First-Nature" and "Second-Nature" Geographies: A Disaggregated Analysis in High-Income Countries. *Glob. Environ. Change* **2020**, *65*, 102167, doi:10.1016/j.gloenvcha.2020.102167.
9. Lal, R.; Delgado, J.A.; Gulliford, J.; Nielsen, D.; Rice, C.W.; Pelt, R.S.V. Adapting Agriculture to Drought and Extreme Events. *J. Soil Water Conserv.* **2012**, *67*, 162A-166A, doi:10.2489/jswc.67.6.162A.
10. Vogel, E.; Donat, M.G.; Alexander, L.V.; Meinshausen, M.; Ray, D.K.; Karoly, D.; Meinshausen, N.; Frieler, K. The Effects of Climate Extremes on Global Agricultural Yields. *Environ. Res. Lett.* **2019**, *14*, 054010, doi:10.1088/1748-9326/ab154b.
11. Below, R.; Grover-Kopec, E.; Dilley, M. Documenting Drought-Related Disasters: A Global Reassessment. *J. Environ. Dev.* **2007**, *16*, 328–344, doi:10.1177/1070496507306222.
12. Vogt, J.V.; Somma, F. *Drought and Drought Mitigation in Europe*; Advances in Natural and Technological Hazards Research; Kluwer Academic Publishers: The Netherlands; ISBN 978-94-015-9472-1.
13. Dracup, J.A.; Lee, K.S.; Paulson, E.G. On the Definition of Droughts. *Water Resour. Res.* **1980**, *16*, 297–302, doi:10.1029/WR016i002p00297.
14. Wilhite, D.A.; Glantz, M.H. Understanding: The Drought Phenomenon: The Role of Definitions. *Water Int.* **1985**, *10*, 111–120, doi:10.1080/02508068508686328.
15. Jonkman, S.N. Global Perspectives on Loss of Human Life Caused by Floods. *Nat. Hazards* **2005**, *34*, 151–175, doi:10.1007/s11069-004-8891-3.
16. López-Moreno, J.I.; Vicente-Serrano, S.M.; Angulo-Martínez, M.; Beguería, S.; Kenawy, A. Trends in Daily Precipitation on the Northeastern Iberian Peninsula, 1955-2006: Trends in Daily Precipitation on the NE Iberian Peninsula. *Int. J. Climatol.* **2010**, *30*, 1026–1041, doi:10.1002/joc.1945.

17. Sánchez, E.; Gallardo, C.; Gaertner, M.A.; Arribas, A.; Castro, M. Future Climate Extreme Events in the Mediterranean Simulated by a Regional Climate Model: A First Approach. *Glob. Planet. Change* **2004**, *44*, 163–180, doi:10.1016/j.gloplacha.2004.06.010.
18. Giorgi, F. Climate Change Hot-Spots. *Geophys. Res. Lett.* **2006**, *33*, doi:10.1029/2006GL025734.
19. Diffenbaugh, N.S.; Pal, J.S.; Giorgi, F.; Gao, X. Heat Stress Intensification in the Mediterranean Climate Change Hotspot. *Geophys. Res. Lett.* **2007**, *34*, doi:10.1029/2007GL030000.
20. Diffenbaugh, N.S.; Giorgi, F. Climate Change Hotspots in the CMIP5 Global Climate Model Ensemble. *Clim. Change* **2012**, *114*, 813–822, doi:10.1007/s10584-012-0570-x.
21. Planton, S.; Lionello, P.; Artale, V.; Aznar, R.; Carrillo, A.; Colin, J.; Congedi, L.; Dubois, C.; Elizalde, A.; Gualdi, S.; et al. The Climate of the Mediterranean Region in Future Climate Projections. In *The Climate of the Mediterranean Region*; Lionello, P., Ed.; Elsevier: Oxford, 2012; pp. 449–502 ISBN 978-0-12-416042-2.
22. Hoegh-Guldberg, O.; Jacob, D.; Taylor, M.; Bindi, M.; Brown, S.; Camilloni, I.; Diedhiou, A.; Djalante, R.; Ebi, K.L.; Engelbrecht, F.; et al. Impacts of 1.5°C of Global Warming on Natural and Human Systems. 138.
23. VICENTE-SERRANO, S.M. Spatial and Temporal Analysis of Droughts in the Iberian Peninsula (1910–2000). *Hydrol. Sci. J.* **2006**, *51*, 83–97, doi:10.1623/hysj.51.1.83.
24. Russo, A.; Gouveia, C.M.; Páscoa, P.; DaCamara, C.C.; Sousa, P.M.; Trigo, R.M. Assessing the Role of Drought Events on Wildfires in the Iberian Peninsula. *Agric. For. Meteorol.* **2017**, *237–238*, 50–59, doi:10.1016/j.agrformet.2017.01.021.
25. Guha-Sapir, D.; Below, R.; Hoyois, P. EM-DAT: The CRED/OFDA International Disaster Database - Www.Emdat.Be. Brussels - Belgium: Université Catholique de Louvain Available online: https://public.emdat.be/ (accessed on 14 April 2021).
26. Santos, J.A.; Pinto, J.G.; Ulbrich, U. On the Development of Strong Ridge Episodes over the Eastern North Atlantic. *Geophys. Res. Lett.* **2009**, *36*, doi:10.1029/2009GL039086.
27. Santos, J.A.; Andrade, C.; Corte-Real, J.; Leite, S. The Role of Large-Scale Eddies in the Occurrence of Winter Precipitation Deficits in Portugal. *Int. J. Climatol.* **2009**, *29*, 1493–1507, doi:10.1002/joc.1818.
28. Santos, J.A.; Woollings, T.; Pinto, J.G. Are the Winters 2010 and 2012 Archetypes Exhibiting Extreme Opposite Behavior of the North Atlantic Jet Stream? *Mon. Weather Rev.* **2013**, *141*, 3626–3640, doi:10.1175/MWR-D-13-00024.1.
29. Woollings, T.; Pinto, J.G.; Santos, J.A. Dynamical Evolution of North Atlantic Ridges and Poleward Jet Stream Displacements. *J. Atmospheric Sci.* **2011**, *68*, 954–963, doi:10.1175/2011JAS3661.1.
30. Lyon, B.; Barnston, A.G. ENSO and the Spatial Extent of Interannual Precipitation Extremes in Tropical Land Areas. *J. Clim.* **2005**, *18*, 5095–5109, doi:10.1175/JCLI3598.1.
31. Lyon, B. The Strength of El Niño and the Spatial Extent of Tropical Drought. *Geophys. Res. Lett.* **2004**, *31*, doi:10.1029/2004GL020901.
32. Andrade, C.; Belo-Pereira, M. Assessment of Droughts in the Iberian Peninsula Using TheWASP-Index. *Atmospheric Sci. Lett.* **2015**, *16*, 208–218, doi:10.1002/asl2.542.
33. Croitoru, A.-E.; Toma, F.-M. Trends in Precipitation and Snow Cover in Central Part of Romanian Plain. *Geogr. Tech.* **2010**, 98.
34. Zubair, L.; Ralapanawe, V.; Tennakoon, U.; Yahiya, Z.; Perera, R. Natural Disaster Risks in Sri Lanka: Mapping Hazards and Risk Hotspots. 28.
35. Lokuhetti, R.; Zubair, L.; Visvanathan, J.; Nijamdeen, A. Drought Monitoring for Sri Lanka: Spatial Extent and Temporal Evolution during the 2016-17 Drought. **2017**.
36. Adnan, S.; Ullah, K.; Shuanglin, L.; Gao, S.; Khan, A.H.; Mahmood, R. Comparison of Various Drought Indices to Monitor Drought Status in Pakistan. *Clim. Dyn.* **2018**, *51*, 1885–1899, doi:10.1007/s00382-017-3987-0.
37. Carrão, H.; Naumann, G.; Barbosa, P. Global Projections of Drought Hazard in a Warming Climate: A Prime for Disaster Risk Management. *Clim. Dyn.* **2018**, *50*, 2137–2155, doi:10.1007/s00382-017-3740-8.
38. Procházka, P.; Hönig, V.; Maitah, M.; Pljučarská, I.; Kleindienst, J. Evaluation of Water Scarcity in Selected Countries of the Middle East. *Water* **2018**, *10*, 1482, doi:10.3390/w10101482.

39. Borgomeo, E.; Vadheim, B.; Woldeyes, F.B.; Alamirew, T.; Tamru, S.; Charles, K.J.; Kebede, S.; Walker, O. The Distributional and Multi-Sectoral Impacts of Rainfall Shocks: Evidence From Computable General Equilibrium Modelling for the Awash Basin, Ethiopia. *Ecol. Econ.* **2018**, *146*, 621–632, doi:10.1016/j.ecolecon.2017.11.038.
40. Ayanlade, S.; Odekunle, T.; Orimoogunje, O.; Adeoye, N. Inter-Annual Climate Variability and Crop Yields Anomalies in Middle Belt of Nigeria. *Appl Sci* **2009**, *3*, 452–465.
41. Cornes, R.C.; Schrier, G. van der; Besselaar, E.J.M. van den; Jones, P.D. An Ensemble Version of the E-OBS Temperature and Precipitation Data Sets. *J. Geophys. Res. Atmospheres* **2018**, *123*, 9391–9409, doi:10.1029/2017JD028200.
42. Moss, R.H.; Edmonds, J.A.; Hibbard, K.A.; Manning, M.R.; Rose, S.K.; van Vuuren, D.P.; Carter, T.R.; Emori, S.; Kainuma, M.; Kram, T.; et al. The next Generation of Scenarios for Climate Change Research and Assessment. *Nature* **2010**, *463*, 747–756, doi:10.1038/nature08823.
43. van Vuuren, D.P.; Edmonds, J.; Kainuma, M.; Riahi, K.; Thomson, A.; Hibbard, K.; Hurtt, G.C.; Kram, T.; Krey, V.; Lamarque, J.-F.; et al. The Representative Concentration Pathways: An Overview. *Clim. Change* **2011**, *109*, 5, doi:10.1007/s10584-011-0148-z.
44. Taylor, K.E.; Stouffer, R.J.; Meehl, G.A. An Overview of CMIP5 and the Experiment Design. *Bull. Am. Meteorol. Soc.* **2012**, *93*, 485–498, doi:10.1175/BAMS-D-11-00094.1.
45. Smith, S.J.; Wigley, T.M.L. Multi-Gas Forcing Stabilization with Minicam. *Energy J.* **2006**, *SI2006*, doi:10.5547/ISSN0195-6574-EJ-VolSI2006-NoSI3-19.
46. Clarke, L.; Edmonds, J.; Jacoby, H.; Pitcher, H.; Reilly, J.; Richels, R. Scenarios of Greenhouse Gas Emissions and Atmospheric Concentrations. 166.
47. Wise, M.; Calvin, K.; Thomson, A.; Clarke, L.; Bond-Lamberty, B.; Sands, R.; Smith, S.J.; Janetos, A.; Edmonds, J. Implications of Limiting CO2 Concentrations for Land Use and Energy. *Science* **2009**, *324*, 1183–1186, doi:10.1126/science.1168475.
48. Rao, S.; Riahi, K. The Role of Non-CO2 Greenhouse Gases in Climate Change Mitigation: Long-Term Scenarios for the 21st Century. *Energy J.* **2006**, *SI2006*, doi:10.5547/ISSN0195-6574-EJ-VolSI2006-NoSI3-9.
49. Riahi, K.; Grübler, A.; Nakicenovic, N. Scenarios of Long-Term Socio-Economic and Environmental Development under Climate Stabilization. *Technol. Forecast. Soc. Change* **2007**, *74*, 887–935, doi:10.1016/j.techfore.2006.05.026.
50. Amengual, A.; Homar, V.; Romero, R.; Alonso, S.; Ramis, C. A Statistical Adjustment of Regional Climate Model Outputs to Local Scales: Application to Platja de Palma, Spain. *J. Clim.* **2012**, *25*, 939–957, doi:10.1175/JCLI-D-10-05024.1.
51. Spinoni, J.; Naumann, G.; Carrao, H.; Barbosa, P.; Vogt, J. World Drought Frequency, Duration, and Severity for 1951–2010. *Int. J. Climatol.* **2014**, *34*, 2792–2804, doi:10.1002/joc.3875.
52. Maccioni, P.; Kossida, M.; Brocca, L.; Moramarco, T. Assessment of the Drought Hazard in the Tiber River Basin in Central Italy and a Comparison of New and Commonly Used Meteorological Indicators. *J. Hydrol. Eng.* **2015**, *20*, 05014029, doi:10.1061/(ASCE)HE.1943-5584.0001094.
53. Caracterização Climática 2003 Caracterização Climática 2003. Instituto Português Do Mar e Da Atmosfera, IPMA 2003. (http://www.ipma.pt/pt/publicacoes/boletins.jsp?cmbDep=cli&cmbTema=pcl&cmbAno=2003&idDep=cli&idTema=pcl&curAno=2003)
54. Caracterização Climática 2004 Caracterização Climática 2004. Instituto Português Do Mar e Da Atmosfera, IPMA 2004. (http://www.ipma.pt/pt/publicacoes/boletins.jsp?cmbDep=cli&cmbTema=pcl&cmbAno=2004&idDep=cli&idTema=pcl&curAno=2004)
55. Vicente-Serrano, S.; Trigo, R.; López-Moreno, J.; Liberato, M.; Lorenzo-Lacruz, J.; Beguería, S.; Morán-Tejeda, E.; El Kenawy, A. Extreme Winter Precipitation in the Iberian Peninsula in 2010: Anomalies, Driving Mechanisms and Future Projections. *Clim. Res.* **2011**, *46*, 51–65, doi:10.3354/cr00977.
56. Ramos, A.M.; Trigo, R.M.; Liberato, M.L.R. A Ranking of High-Resolution Daily Precipitation Extreme Events for the Iberian Peninsula: Ranking of the Iberian Peninsula Daily Precipitation. *Atmospheric Sci. Lett.* **2014**, doi:10.1002/asl2.507.

57. Spinoni, J.; Barbosa, P.; De Jager, A.; McCormick, N.; Naumann, G.; Vogt, J.V.; Magni, D.; Masante, D.; Mazzeschi, M. A New Global Database of Meteorological Drought Events from 1951 to 2016. *J. Hydrol. Reg. Stud.* **2019**, *22*, 100593, doi:10.1016/j.ejrh.2019.100593.
58. Andrade, C.; Leite, S.M.; Santos, J.A. Temperature Extremes in Europe: Overview of Their Driving Atmospheric Patterns. *Nat. Hazards Earth Syst. Sci.* **2012**, *12*, 1671–1691, doi:10.5194/nhess-12-1671-2012.
59. Andrade, C.; Fraga, H.; Santos, J.A. Climate Change Multi-Model Projections for Temperature Extremes in Portugal. *Atmospheric Sci. Lett.* **2014**, *15*, 149–156, doi:10.1002/asl2.485.
60. Merino, A.; Fernández-Vaquero, M.; López, L.; Fernández-González, S.; Hermida, L.; Sánchez, J.L.; García-Ortega, E.; Gascón, E. Large-Scale Patterns of Daily Precipitation Extremes on the Iberian Peninsula: PRECIPITATION EXTREMES ON THE IBERIAN PENINSULA. *Int. J. Climatol.* **2016**, *36*, 3873–3891, doi:10.1002/joc.4601.
61. Spinoni, J.; Vogt, J.V.; Naumann, G.; Barbosa, P.; Dosio, A. Will Drought Events Become More Frequent and Severe in Europe? *Int. J. Climatol.* **2018**, *38*, 1718–1736, doi:10.1002/joc.5291.
62. Andrade, C.; Contente, J. Climate Change Projections for the Worldwide Bioclimatic Classification System in the Iberian Peninsula until 2070. *Int. J. Climatol.* **2020**, 1–24, doi:10.1002/joc.6553.
63. Andrade, C.; Contente, J. Köppen's Climate Classification Projections for the Iberian Peninsula. *Clim. Res.* **2020**, *81*, 71–89, doi:10.3354/cr01604.
64. Kamali, B.; Houshmand Kouchi, D.; Yang, H.; Mikayilov, F. Multilevel Drought Hazard Assessment under Climate Change Scenarios in Semi-Arid Regions—A Case Study of the Karkheh River Basin in Iran. *Water* **2017**, *9*, doi:10.3390/w9040241.
65. Santos, J.A.; Belo-Pereira, M.; Fraga, H.; Pinto, J.G. Understanding Climate Change Projections for Precipitation over Western Europe with a Weather Typing Approach. *J. Geophys. Res. Atmospheres* **2016**, *121*, 1170–1189, doi:10.1002/2015JD024399.
66. Santos, M.; Fragoso, M.; Santos, J.A. Regionalization and Susceptibility Assessment to Daily Precipitation Extremes in Mainland Portugal. *Appl. Geogr.* **2017**, *86*, 128–138, doi:10.1016/j.apgeog.2017.06.020.
67. Santos, M.; Fragoso, M.; Santos, J.A. Damaging Flood Severity Assessment in Northern Portugal over More than 150 Years (1865–2016). *Nat. Hazards* **2018**, *91*, 983–1002, doi:10.1007/s11069-017-3166-y.
68. Santos, M.; Fonseca, A.; Fragoso, M.; Santos, J.A. Recent and Future Changes of Precipitation Extremes in Mainland Portugal. *Theor. Appl. Climatol.* **2019**, *137*, 1305–1319, doi:10.1007/s00704-018-2667-2.
69. Carrão, H.; Naumann, G.; Barbosa, P. Climate Change Impacts on Droughts. 2016.
70. Yang, C.; Fraga, H.; van Ieperen, W.; Santos, J.A. Assessing the Impacts of Recent-Past Climatic Constraints on Potential Wheat Yield and Adaptation Options under Mediterranean Climate in Southern Portugal. *Agric. Syst.* **2020**, *182*, 102844, doi:10.1016/j.agsy.2020.102844.
71. Molitor, D.; Fraga, H.; Junk, J. UniPhen – a Unified High Resolution Model Approach to Simulate the Phenological Development of a Broad Range of Grape Cultivars as Well as a Potential New Bioclimatic Indicator. *Agric. For. Meteorol.* **2020**, *291*, 108024, doi:10.1016/j.agrformet.2020.108024.
72. Fraga, H.; Pinto, J.G.; Santos, J.A. Olive Tree Irrigation as a Climate Change Adaptation Measure in Alentejo, Portugal. *Agric. Water Manag.* **2020**, *237*, 106193, doi:10.1016/j.agwat.2020.106193.